UNIVERSIDAD CATÓLICA DEL NORTE

FACULTAD DE CIENCIAS

Departamento de Física

AGN variability observed with the VYSOS6 telescope on Cerro Armazones

Tesis para optar al grado de Magíster en Ciencias con mención en Física y Astronomía.

Lic.Francisco Pozo Nuñez

Profesor Guía: Dr.Rolf Chini, Dr.Martin Haas

Antofagasta, Chile

2011

Acknowledgements

First of all I would like to thank my supervisor, Prof. Dr. Rolf Chini, for accepting me as his student in Chile, allowing me to participate in his Astrophysics research group. Many thanks for making possible my research stay in Germany and for all the time dedicated to the supervision of this work.

I am also grateful my advisor, Dr. Martin Haas, scientist in Prof. Rolf Chini's team for Astrophysics at the Ruhr-University Bochum and head of the research group Active Galactic Nuclei and Quasars. He has supervised me since the first days of my thesis work, introducing and guiding me in the AGN research field and always responding to my questions with many ideas and suggestions. Really, thank you very much for all the dedicated time. Special thanks to Dr. Miguel Murphy, who motivated me to continue my studies in astronomy. Thank you very much for all the advice, discussions and for always making the necessary preparations for the visits to the Armazones Observatory.

I would also like to thank Michael Ramolla for all his help during my thesis work and my stay at the Astronomisches Institut Ruhr-Universität Bochum (AIRUB). Many thanks to Christian Westhues (AIRUB) for the discussion about my work and IDL. Special thanks Doris Hasinger for all the help provided and her concern during my stay in AIRUB.

I also deeply have to thank Katrien Steenbrugge for all their corrections in this work and his advices to improve my usage of the english language.

Finally, a great thank you to my family, my girlfriend Angie and friends for the unconditional support they have always given me.

Abstract

In this thesis I present new monitoring results of three local active galactic nuclei (AGNs), 3C120, Ark120 and PG0003+199 observed with the robotic 15cm telescope VYSOS6 on Cerro Murphy, Chile. Broad line region (BLR) sizes, Black hole masses (BH) and the galaxy host subtracted luminosities were determined with photometric reverberation mapping and applying the Flux Variation Gradient (FVG) method. While spectroscopic reverberation mapping is a expensive technique, the aim of the presented study is to establish a more efficient photometric reverberation mapping method and to compare the results with those obtained using the spectroscopic reverberation data available.

Observations in broad (B, V) and narrow band ($SII, OIII$) filters were performed in order to measure the variations in the continuum and the time lag (echo) of the BLR emission lines respectively. For 3C120 and Ark120 the narrow band is constituted by about 50% continuum emission and 50% $H\beta$ line emission. To obtain the time lag of only the emission line, I create a synthetic $H\beta$ light curve by subtracting a scaled V-band light curve from the narrow-band light curve. For PG0003+199 the narrow band contains about 85% of the $H\alpha$ emission line, and thus the time lag can be obtained without subtracting the continuum contribution. The median sampling of 2 days enabled us to achieve exceptionally small errors of about 10% in the lags obtained from the cross correlation of the light curves. Virial black hole mass calculations are consistent with previous results in the literature. The host-subtracted rest-frame 5100$\AA$ luminosity was determined with an uncertainty of about 10%. These results allow us to re-examine and improve the R_{BLR}-L relationship.

Contents

List of Figures

List of Tables

Chapter 1

Optical continuum color contribution in Active Galactic Nuclei

1.1 Introduction

Since their discovery (1960-1970), several studies have been conducted to try understand the nature of the strong variability observed in active galactic nuclei (AGN). Most of these attempts have focused on short and long term photometric and spectroscopic monitoring, covering the electromagnetic spectrum from radio waves to X-rays. Different models have been proposed to explain the physical origin of this peculiar and variable radiation. These include instability in the accretion disk (Rees 1984, Kawaguchi et al. 1998), Supernovae events (Aretxaga et al. 1995) and gravitational microlensing (Paczynski 1986; Schneider 1987; Schneider 1993; Hawkins 1993; Hawkins 2002).

Each of the models mentioned are based on different physical mechanisms and thus the fundamental mechanism that causes the observed variability is still unknown.

It is generally believed that the variability is related the accretion and emission processes ocurring in the vicinity of the black hole. This means that to probe the origin we need to observe the immediate surroundings of the central engine. This theory thus requires that we can differentiate between the light from the central engine and that of the host galaxy.

The first method to determine the nuclear flux contribution with respect to the total light emitted (i.e. including the host galaxy) was developed by Sandage (1973). He assumed a two component model: a giant elliptical galaxy and a source considered to be a quasi stellar point. This model model gives a realistic first approximation of both components, i.e. the host galaxy and nucleus.

A big improvement step forward in determining the optical nuclear flux contribution was obtained by Cholonieswki (1981), who proposed that the respective fluxes are determined using the flux to flux diagram, also called the flux variation gradient method FVGs (Winkler et al. 1992). This model, similar to the method proposed by Sandage (1973) considers two components:the combination of the non-variable subcomponents and variable component. The non-variable subcomponent includes emission from 1) the stars in the host galaxy, 2) The continuum emission. 3) The thermal emission of the dust heated by the non-thermal variable source. The variable component includes 1) the innermost part of the AGN and which is supposed to have a non-thermal emission nature and 2) thermal emission from the dust torus. Choloniewski (1981) found that despite of the strong variability in the observed flux, the energy distribution in the spectrum of the variable component remains constant, thus the color index from the non-thermal variable radiation remains constant too.

In this work I present a new monitoring observation of two Seyfert 1 galaxies 3C120 and Ark120. The flux variation gradient method is used to separate the AGN luminosity from the contribution of the host galaxy. Both objects have published monitoring and which allows us to establish the quality of our results before starting to monitor of other less well known AGN using the VYSOS6 telescope.

In section 1.2 we describe the observations, data reduction and the applied photometry. In section 1.3 we review the flux variation gradient method (FVG). In section 1.4, 1.5 and 1.6 we present the optical flux variability of both Seyfert galaxies and discuss the color variability using a linear correlation between the fluxes obtained. In section 1.7 we discuss the variable optical continuum component, and compare it with the non-variable host galaxy component. We also summarize our results.

1.2 Observations and data reduction

Johnson-Cousins B and V photometric observations were made with the robotic 15 cm VYSOS6 telescope of the Universitätssternwarte Bochum, Germany. This telescope is placed on Cerro Murphy in the Chilean Atacama desert, close to the site where the European Extremely Large Telescope (E-ELT) will be build. This site has excellent observing conditions and is well suited for short-and long-term monitoring programs. The sources were monitored between October 2009 and February 2010 using the Apogee Alta U16M CCD camera, which has a pixel size of 9 microns, an array of 4096×4096 pixels, a pixel scale of 2.37"/pix and a field of view of $2°42' \times 2°42'$.

The VYSOS6 telescope has the ability to acquire images in the optical BVRI-bands controlled remotely by the Astronomisches Institut Ruhr-Universität Bochum (AIRUB hereafter) by using highly automated pipeline observing system (Watermann, R. 2011).

The data reduction was performed using BOVIP routine (**B**ochum **V**YSOS **I**nteractive **P**ipeline) developed by Martin Haas (AIRUB) following standard image reduction such as subtraction of the appropriate bias and sky flat field.

The SCAMP routine was used to find the WCS coordinates for each pixel on the frames. This routine compares the position of all sources in the images, previously identified by SExtractor, with the 2MASS catalogue with a precision of about 0.1" per pixel. Each original image, with an scale of 2.37" per pixel, was resampling to 0.75" per pixel using the SWarp routine, in order to obtain a higher resolution and avoid problems of distortion produced by diffraction effects in the telescope's projection. The 5-9 images taken during a night were combined after bad pixels and cosmic rays were rejected into a final image with a higher signal to noise ratio. All final images were aligned at the same WCS coordinates using the IRAF[1] routine IMALIGN. Afterwards, the photometry was determined automatically.

For the photometry analysis we used DAOPHOT (IRAF) and SExtractor combined with IPIP (**I**RAF **P**hotometry **I**nteractive **P**ipeline) routine (F.Pozo 2011). The comparison between the photometry realized with DAOPHOT and SExtractor give consistent results.

[1]IRAF (Image Reduction and Analysis Facility) is distributed by the National Optical Astronomy Observatories, which are operated by AURA, Inc., under cooperative agreement with the National Science Foundation.

Table 1.1. Description of the sample and observational information.

Name	other name	α (2000)	δ (2000)]	z	D_L	$A_B{}^{(1)}$	$A_V{}^{(1)}$
					(Mpc)	(mag)	(mag)
Ark120	Mrk 1095	05:16:11.421	-00:08:59.380	0.03271	141.8	0.554	0.426
3C120	Mrk 1506	04:33:11.095	+05:21:15.620	0.03301	145.0	1.283	0.986

Note. — (1)Values used to correct for galactic extinction in B and V band from Schlegel et al. 1998.

The optimal photometric aperture was determined using the APCALC routine from the VAPHOT package (Deeg, HJ & Doyle 2001). This is a iterative routine determining the optimal aperture by maximizing the signal to noise ratio (Howell, 1989). As a comparison we determined the B and V bands fluxes for each AGN and nearby reference stars located on the same field within 30' around the AGN and of similar brightness using an aperture of 5", 7.5", 15" and 25".

Normalized flux density light curves were constructed and subsequently averaged to obtain the final light curve in each aperture. The calibrated magnitudes light curves were obtained using the measured fluxes of references stars from SA092, SA095 and SA111 fields (A. Landolt 2009). The calibrated magnitudes were converted into absolute fluxes by using the respective zero point fluxes of calibration. Light curves for 3C120, Ark120 and for two reference stars are presented in Fig (1.1) - (1.4) respectively. The source parameters are summarized in Tab (1.1).

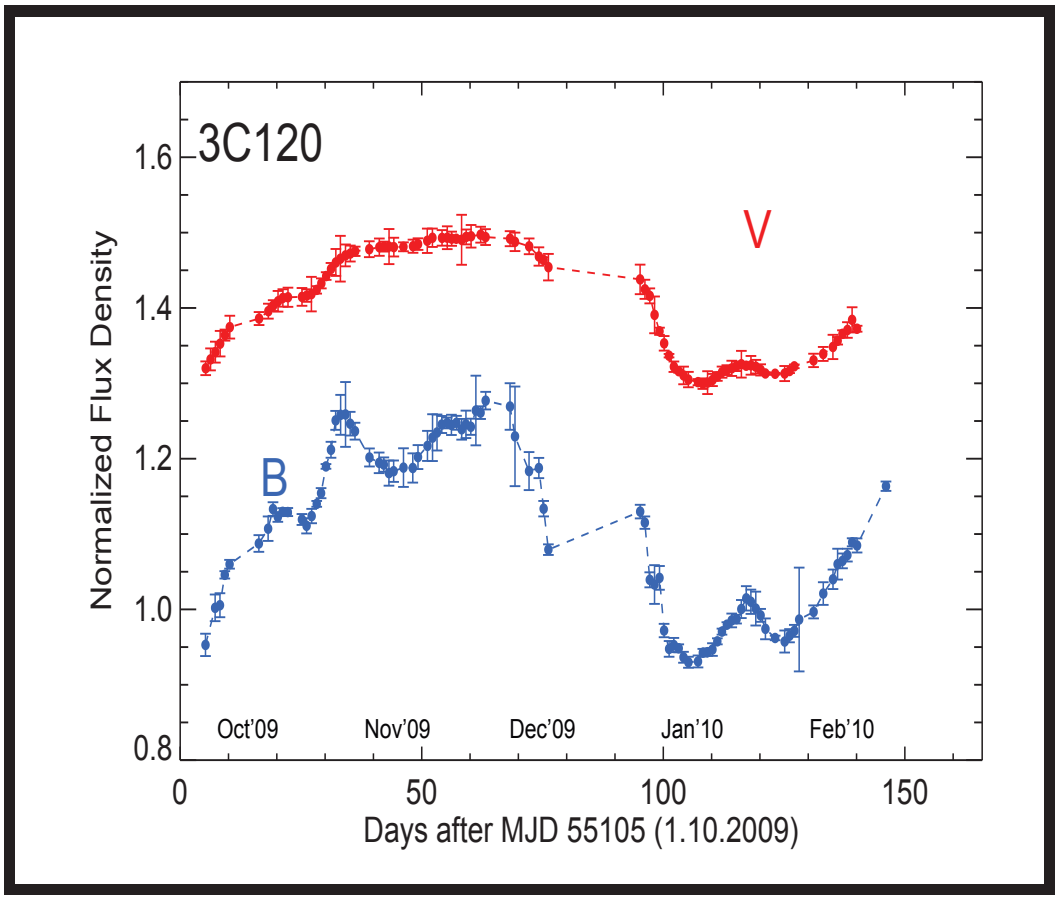

Figure 1.1 .B-band and V-band light curves for 3C120, observed between October 2009 and March 2010.

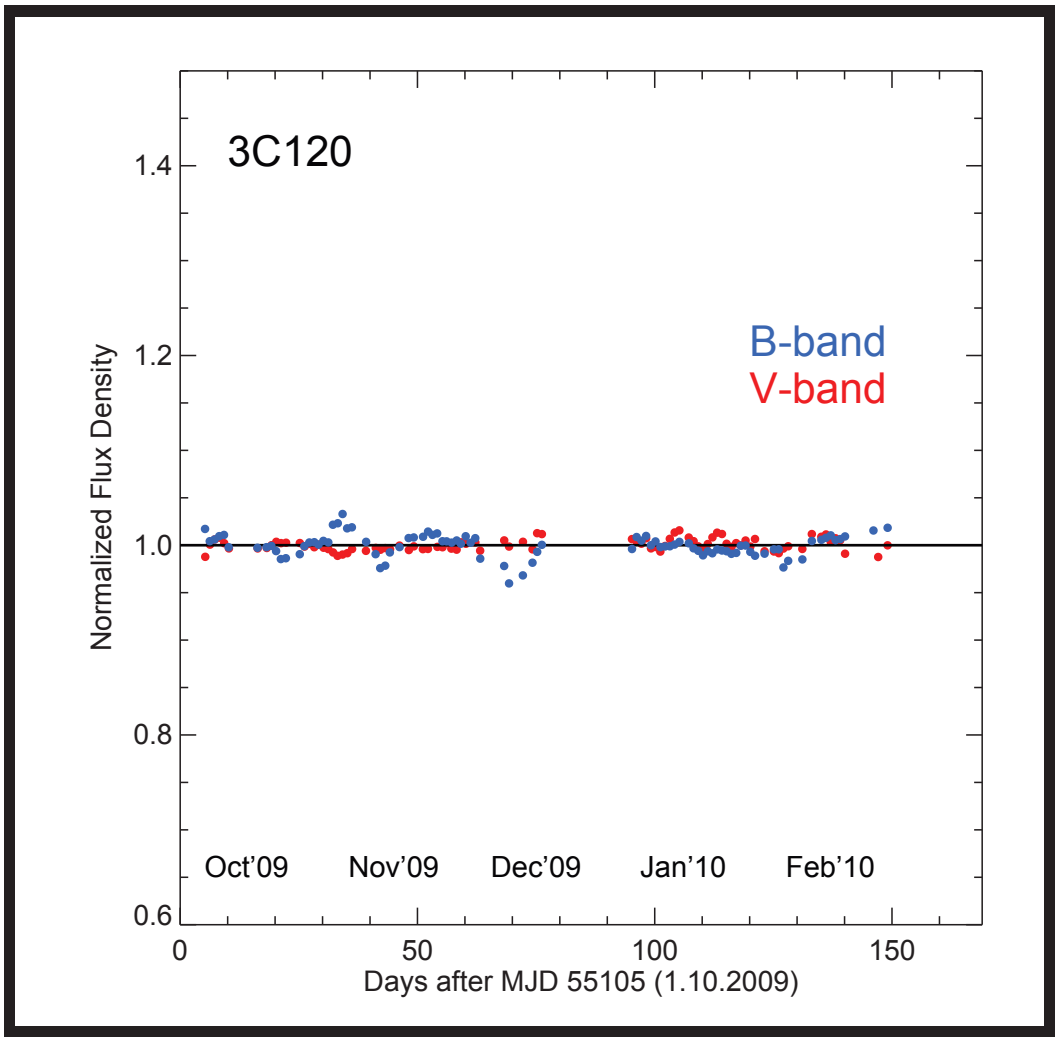

Figure 1.2 B-band and V-band light curves for two references stars on the field of 3C120.

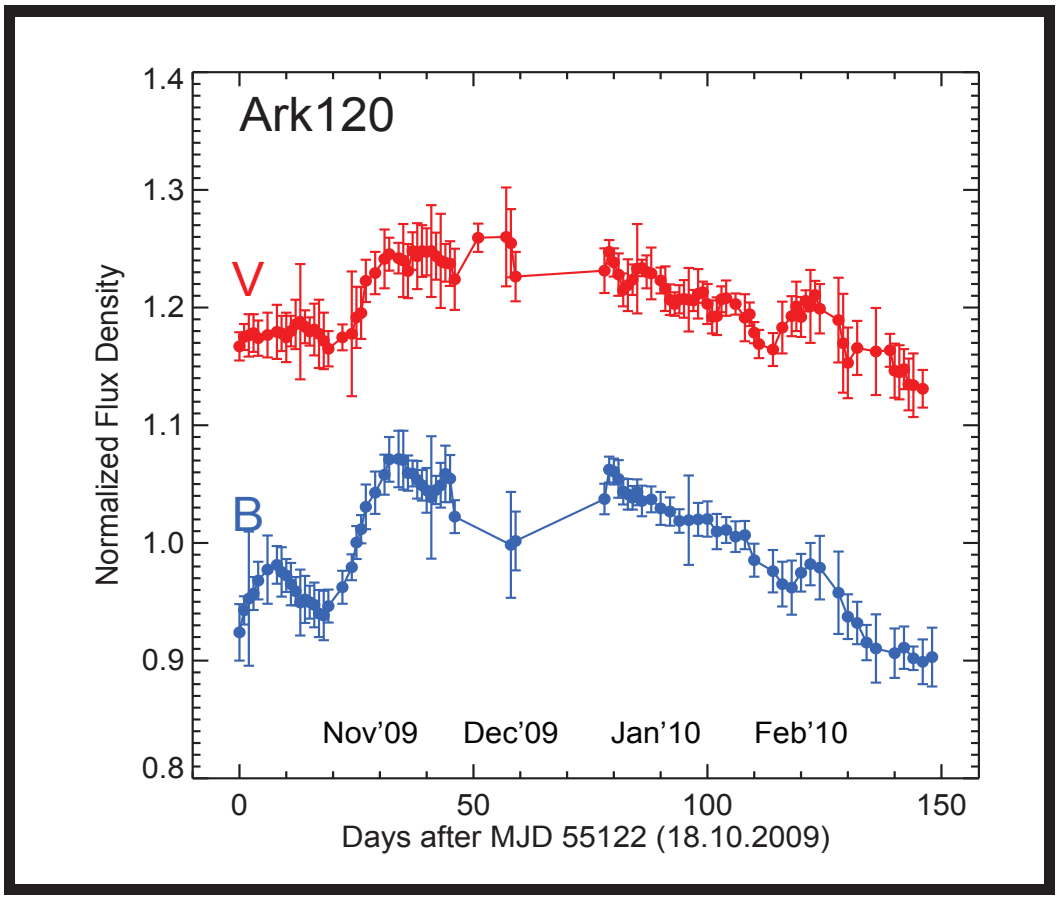

Figure 1.3 .B-band and V-band light curves for Ark120, observed between October 2009 and March 2010.

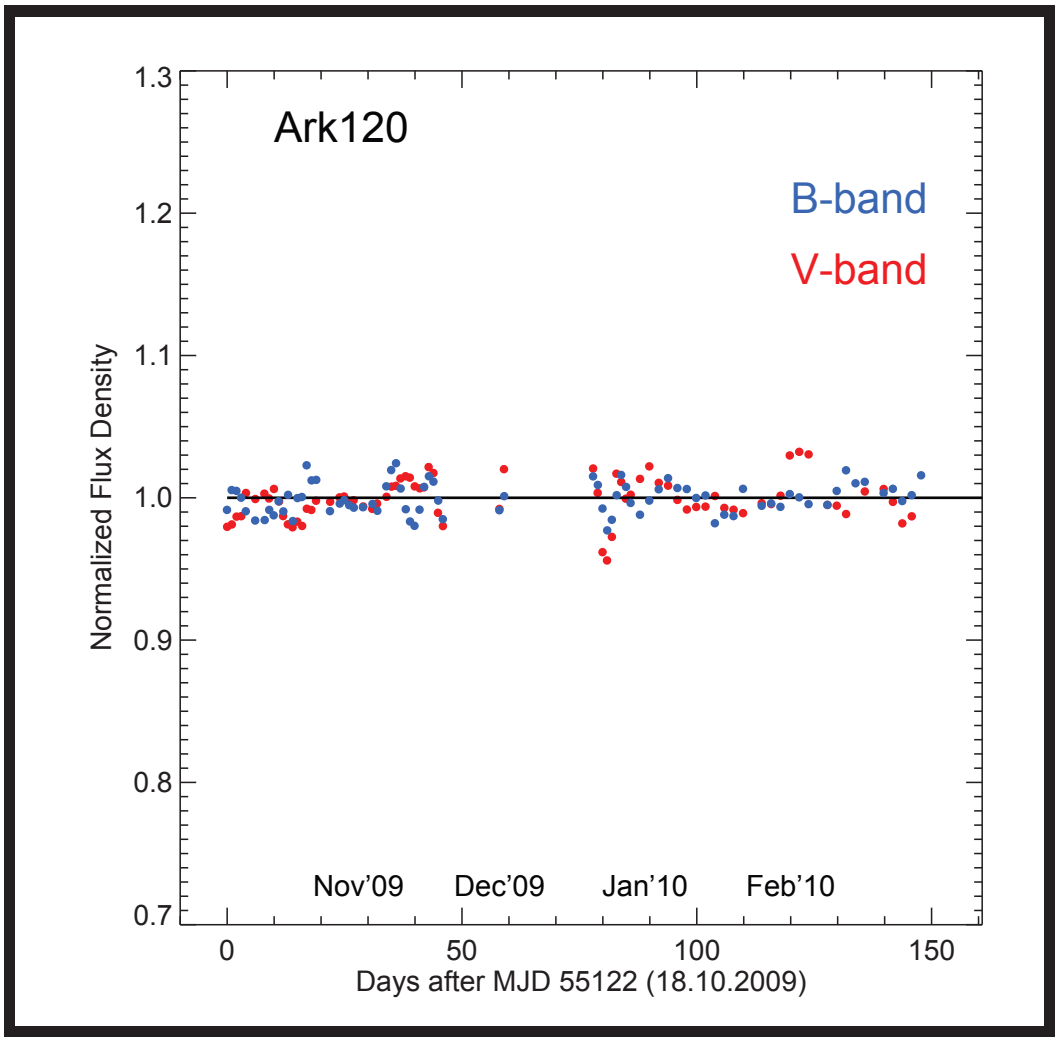

Figure 1.4 B-band and V-band light curves for two references stars on the field of Ark120.

1.3 Review of the flux variation gradient method (FVG)

The effect of the the nuclear continuum color with respect to the host galaxy emission in AGNs, was first discussed by Choloniewski (1981). Choloniewski noticed a linear relationship between the fluxes obtained in two differents filters taken at different epochs. Using this relationship he demonstrated the existence of two component structure to the spectra of Seyfert galaxies.

The two component structure assumes that one component is constant in time and that the second component has a strong variability, but that despite of this strong variability the spectral energy distribution (SED) does not change. Choloniewski(1981) plotted the observed UVB fluxes for 40 Seyfert galaxies as 3 dimensional vectors. This gave a clear geometrical interpretation of the total flux and allowed for the decomposition of the total vector flux $\vec{\phi}(t)$ in a constant vector $\vec{F}$ and another variable vector $\vec{f}(t)$, see Fig (1.5).

The $(\vec{\phi}_U, \vec{\phi}_B)$ plane, can be generalized to an n-dimensional case, due to the fact we can reduce an n-dimensional representation to the plane through projection onto the $(\vec{\phi}_i, \vec{\phi}_j)$ plane. Therefore, it suffices to consider only the two-dimensional case (Hagen-Thorn 1995). Following the geometrical representation from Choloniewski (1981), we can write the two component structure using two different filters as:

$$\vec{\phi}_{i,j}(\nu, t) = \vec{F}_{i,j}(\nu) + \vec{f}_{i,j}(\nu, t) \tag{1.1}$$

where the observed flux $\vec{F}_{i,j}(\nu)$ and $\vec{f}_{i,j}(\nu, t)$ are the constant and variable components in two arbitrary filters respectively.

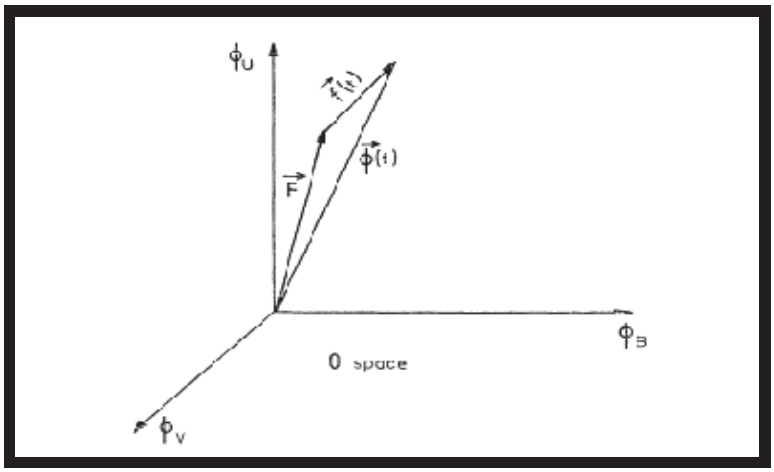

Figure 1.5 .Vectors $\vec{\phi}(t)$, $\vec{F}$ and $\vec{f}(t)$ in the three dimensional space from Choloniewski(1981).

Assuming that the shape of spectrum of the variable component does not change, one deduces:

$$\frac{\vec{f_j}(\nu,t)}{\vec{f_i}(\nu,t)} = a_{ji} \tag{1.2}$$

where a_{ji} is a constant. Using equations (1.1) y (1.2) we obtain the equation of a straight line in the plane ($\vec{\phi_i}$, $\vec{\phi_j}$):

$$\vec{\phi_j}(\nu,t) = a_{ji}\vec{\phi_i}(\nu,t) + b_{ji} \tag{1.3}$$

where $b_{ji} = \vec{F_j}(\nu) - a_{ji}\vec{F_i}(\nu)$

Thus the coefficient a_{ji} represents the color index of the variable component (assuming that the energy distribution of the variable source is unchanged) and the value of which depends on the individual Seyfert galaxy. This coefficient of proportionality has also been called the flux variation gradient (FVG) and is

denoted by the symbol Γ by Winkler et al. (1992). Both, a_{ji} and b_{ji} coefficients have to be determined by a linear regression analysis.

The choice of which regression method to use is not an easy task. The method depends on the degree of knowledge about the data, especially on how well separeted the dependent and independent variables are, the measurement errors, the intrinsic dispersion of data around the best fit and others factors (Isobe et al. 1990).

Winkler et al. (1992) proposed a new method to separate the nuclear flux from the host galaxy, based on the flux-flux diagrams implemented by Choloniewski (1981). Winkler monitored 35 southern Seyfert galaxies using UBVRI multi-aperture photometry to estimate the colors of the host galaxy. He plotted the total fluxes obtained through $20''$ and $30''$ aperture, together with a line representing the fluxes from a one component having the same colors as the host galaxy. The intersection of this line with the linear regression fit obtained from the total flux represents then the contribution from the host galaxy at the time or epoch of each observation, see Fig (1.6).

The nuclear flux is then calculated by subtracting the constant host galaxy component (obtained by the FVGs method) from the total flux. In the same way as Cholonieswki (1981), Winkler et al. (1992) determined the nuclear color, i.e. the color of the variable component by converting the fluxes into magnitudes.

As a result of the studies by Choloniewski (1981) and Winkler et al. (1992) it was observationally established that the variable component has a constant blue color and becomes brighter increasing over the non-variable component, which is reddened[2], see Fig (1.7).

[2]Typical intrinsic colors of a Seyfert nucleus $V - I = 0.35 \pm 0.10$.

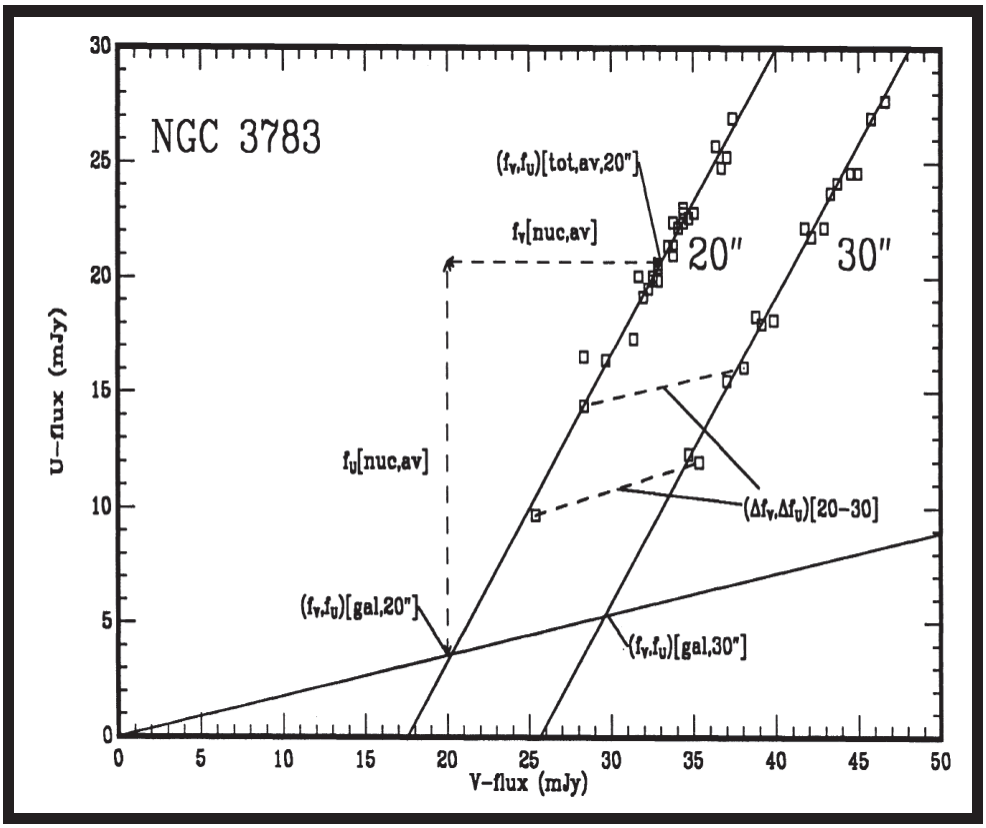

Figure 1.6 .Plot of U versus V flux of NGC3783 from Winkler(1992). It can be readily seen that the method does not work if the colors of the nucleus and host galaxy are similar.

A recent study on the determination of the nuclear flux contribution was realized by Sakata et al. (2010). In this study the flux of the host galaxy was estimated for 11 nearby Seyfert galaxies and QSOs. These fluxes were measured in B, V and I bands by using surface brightness fitting to the high resolution Hubble Space Telescope (HST) images and from the MAGNUM telescope observations. The authors find a well defined range for the host galaxy slope of $0.4 < \Gamma_{BV}^{host} < 0.53$, which corresponds to host galaxy colors of $0.8 < B - V < 1.1$. These results are consistent with those obtained by Winkler et al. (1992) and Winkler (1997).

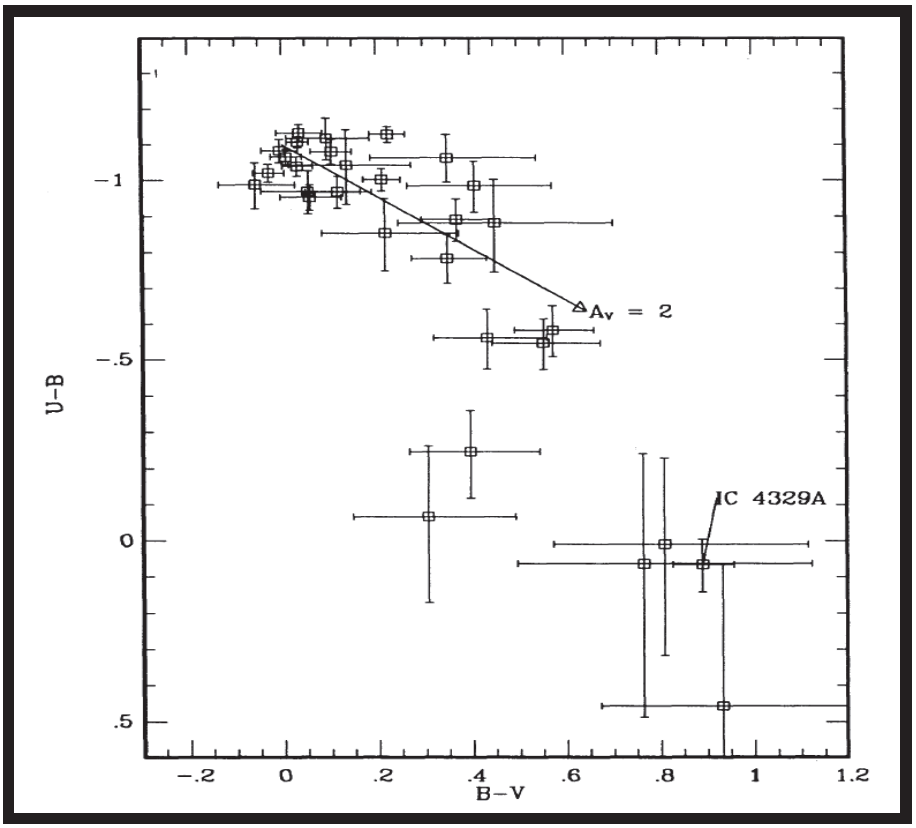

Figure 1.7 $.U - B$ versus $B - V$ plot of the nuclear colors from Winkler(1992), a similar plot for B-V versus V-I can be seen in Winkler(1992). The typical intrinsic color was $B - V = 0.00 \pm 0.03$.

The studies conducted to date by Choloniewski (1981), Winkler et al. (1992) and Sakata et al. (2010) have shown that the slope of the AGN is constant. From observations with HST we know that the contribution of the host galaxy lies on the faint end of the slope. In this work we use the FVG method and the well defined range of host colors determined from previous investigations. This method is presented here as a feasible and efficient alternative to determine the host-subtracted AGN luminosities.

1.4 Analysis of Data

As a first step we analyze the color indices using the total flux (host+nucleus) for both Seyfert 1 galaxies. We observe that on average as the total brightness increases, the color index decreases. Thus the color of the total flux becomes bluer as the flux of the nucleus increases.

Using the established interpretation that the variable component is variable but maintains a constant SED, we have plotted B and V total flux obtained during the same nights and through the same aperture in a flux-flux diagram (e.g. Choloniewski 1981, Winkler et al. 1992, Winkler 1997). The total flux contains a contribution due to the emission lines emitted in the narrow line region (NLR), however, this contribution is less than 10% of the host galaxy flux in the B and V band (Sakata et al. 2010).

Flux Variations Gradients (FVGs) were evaluated by fitting a straight line to the data using five methods of linear regression; OLS(Y/X), OLS(X/Y), OLS bisector, Orthogonal regression and Reduced major-axis were used, depending on the corresponding error treatment for each method. The straight line fitting to the data was realized through code from author and which is based on the linear regression formulas given by Isobe (1990).

1.5 3C120

The Seyfert 1 galaxy 3C120 (redshift $z = 0.0331$) is known to be strongly variable in the optical, characterized by short and long term variations with amplitudes of up 2 mag on a timescale of 10 years (Lyutyi 1979, Webb 1988). Subsequent studies showed amplitude variations of about 0.4 mag (Winkler et al. 1997) and 1.5 mag (Sakata et al. 2010) on a timescale of 4 years monitoring. This large amplitude variability makes 3C120 an interesting object for variability studies.

1.5.1 The host galaxy flux determination

Through multi-color surface brightness fitting photometry Barway et al. (2005) have determined the host colour of 3C120 (designated as UGC3087 in figure 2 of Barway et al. 2005) to be $B - V = 1.0$. Using a decomposition of the MAGNUM telescope images into two components, one for the AGN and other for the host galaxy, Sakata et al. (2010) have determined, by doing aperture photometry on this AGN nucleus free images, that the host galaxy colour have a value of $B - V = 0.79$. This small range of host galaxy color allows us to determine the host galaxy contribution at the time of our observations.

Fig (1.8) shows the B versus V flux diagram for the different apertures used in our analysis. All data were corrected for Galactic foreground extinction using the values determined by Schlegel et al. (1998). The solid lines represent the best-fit regression model and yield the range in the slope of the AGN for each aperture. The dotted lines represent the range in the slope for the host galaxy as given by Sakata et al. (2010) and Barway et al. (2005). The intersection between the host galaxy and AGN slope gives the host galaxy flux in both bands. In the figure the shaded, differently colored areas represent the range in acceptable fits for the different apertures used.

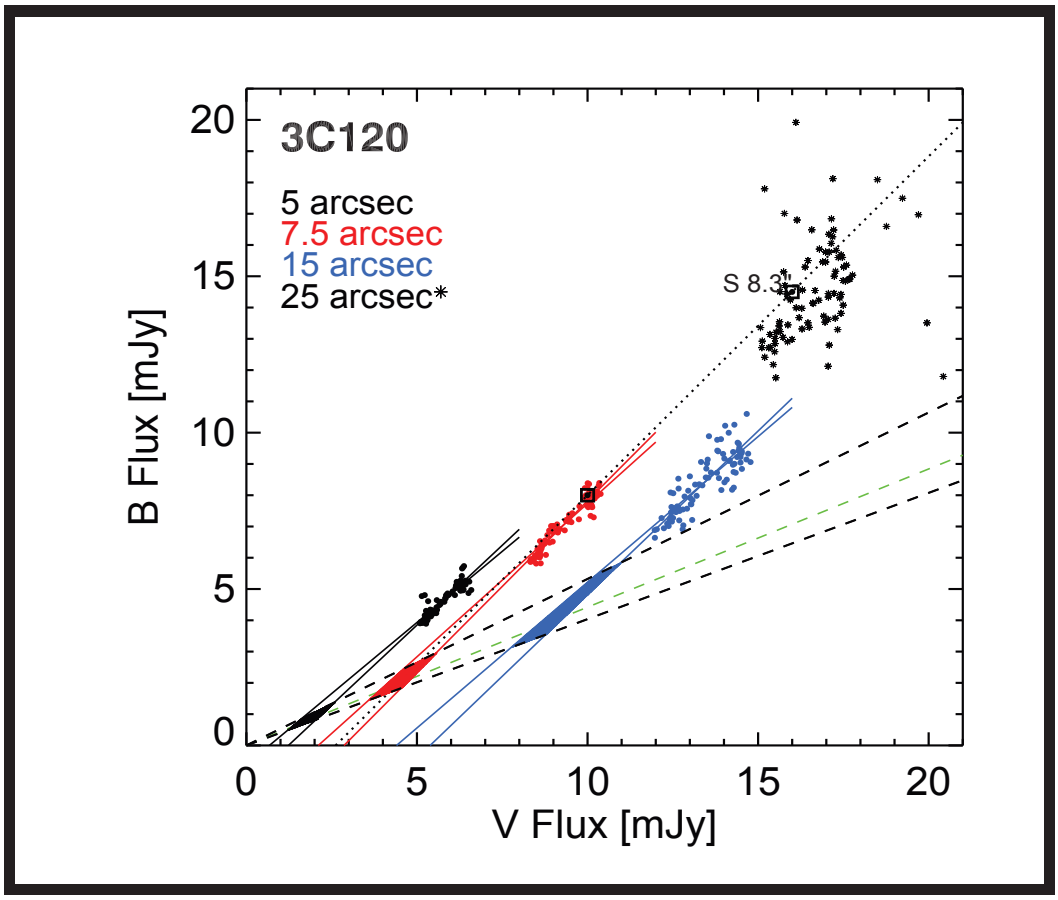

Figure 1.8 . B versus V fluxes of 3C120, measured with different apertures.

The black, red and blue points correspond to the 5", 7.5", and 15" of aperture diameter respectively, and for clarity 25" results correspond to the star symbol in black. The two open squares represent the range of fluxes obtained by Sakata et al. (2010) using a 8.3" aperture on the MAGNUM images and the dotted line through these points correspond to the AGN slope fit.

The results obtained using the different apertures differs considerably. We find that an aperture of 7.5" maximizes the signal to noise ratio (see our previous description of APCALC) and result in a larger correlation in both bands.

From Fig (1.8) it is clear that the other apertures introduce more scatter in the relation. The results obtained for each aperture and linear regression analysis are listed in Tab (1.2) and Tab (1.3) respectively.

For comparison with the results from Sakata et al. (2010) we redid the analysis for an aperture of 8.3" like in Sakata et al. (2010), but the results were similar to those obtained with 7.5". 3C120 was thus clearly weaker during our monitoring campaign.

Using the 7.5" aperture as the best aperture photometry, the best-fit regression line yields a linear gradient of $\Gamma_{BV} = 1.12 \pm 0.04$ and which define the range of the AGN slope. This result is consistent with $\Gamma_{BV} = 1.11 \pm 0.02$ determined by Sakata et al. (2010) and $\Gamma_{BV} = 1.02 \pm 0.07$ determined by Winkler (1997). Averaging over the intersection area between the AGN and the host galaxy slopes, we have obtained a mean host galaxy flux of 2.33 ± 0.28 mJy in B and 4.73 ± 0.36 mJy in V, which represent a contribution of about 50% in V and about 31% in B band with respect to the total flux. These results are consistent with the values $fB \approx 2.10$ mJy and $fV \approx 4.73$ mJy obtained by Sakata et al. (2010) considering the flux contribution of the narrow lines in each filter (his Table 7).

Table 1.2. Photometry results of 3C120 for each aperture

Name	Date	aperture [arcsec]	B [mag]	σ_B	V [mag]	σ_V	$fB_{total}[mJy]$	$fV_{total}[mJy]$
$3C120$	$October.2009 - March.2010$	5	$14.68 - 15.10$	$0.021 - 0.014$	$14.41 - 14.69$	$0.010 - 0.010$	4.63 ± 0.10	5.76 ± 0.10
		7.5	$14.27 - 14.66$	$0.010 - 0.010$	$13.92 - 14.18$	$0.014 - 0.029$	7.02 ± 0.11	9.27 ± 0.10
		8.3	$14.20 - 14.57$	$0.010 - 0.010$	$13.85 - 14.09$	$0.020 - 0.028$	7.51 ± 0.12	9.92 ± 0.10
		15	$14.01 - 14.52$	$0.021 - 0.062$	$13.54 - 13.76$	$0.022 - 0.020$	8.42 ± 0.26	13.44 ± 0.18
		25	$13.33 - 13.90$	$0.086 - 0.040$	$12.99 - 13.51$	$0.128 - 0.020$	14.51 ± 0.62	16.89 ± 0.38

Note. — All data were corrected for galactic foreground extinction using the values determined by Schlegel et al. (1998). fB_{total} and fV_{total} refer to the mean of the total flux ranges during our monitoring campaigns.

Table 1.3. Linear regression results for 3C120

Name	aperture [arcsec]	method	a^a	σ_a	b^b	σ_b
$3C120$	5	$OLS(X/Y)$	0.97	0.06	−0.94	0.32
	5	$OLS(Y/X)$	1.15	0.05	−2.01	0.29
	5	OLS Bisector	1.05	0.05	−1.45	0.27
	5	*Orthogonal Regression*	1.06	0.05	−1.48	0.30
	5	RMA	1.05	0.05	−1.45	0.27
	7.5	$OLS(X/Y)$	1.04	0.06	−2.60	0.53
	7.5	$OLS(Y/X)$	1.21	0.05	−4.22	0.33
	7.5	OLS Bisector	1.12	0.04	−3.38	0.39
	7.5	*Orthogonal Regression*	1.13	0.05	−3.48	0.41
	7.5	RMA	1.12	0.04	−3.38	0.39
	8.3	$OLS(X/Y)$	1.12	0.04	−3.58	0.43
	8.3	$OLS(Y/X)$	1.26	0.03	−4.98	0.35
	8.3	OLS Bisector	1.19	0.03	−4.26	0.34
	8.3	*Orthogonal Regression*	1.20	0.04	−4.38	0.35
	8.3	RMA	1.19	0.03	−4.26	0.34
	15	$OLS(X/Y)$	0.99	0.06	−4.87	0.77
	15	$OLS(Y/X)$	1.36	0.08	−9.83	1.10
	15	OLS Bisector	1.16	0.06	−7.12	0.79
	15	*Orthogonal Regression*	1.19	0.07	−7.55	0.97
	15	RMA	1.16	0.06	−7.15	0.81
	25	$OLS(X/Y)$	0.08	0.17	13.23	2.82
	25	$OLS(Y/X)$	13.98	27.08	−221.63	477.95
	25	OLS Bisector	1.00	0.06	−2.45	0.59

Table 1.3 (continued)

Name	aperture [arcsec]	method	a^a	σ_a	b^b	σ_b
	25	*Orthogonal Regression*	1.48	2.85	−10.41	43.31
	25	*RMA*	1.03	0.19	−2.88	3.30

Note. — Linear regression results for OLS(X/Y), OLS(Y/X), OLS Bisector, Orthogonal Regression and the Reduced Major Axis methods. (a)Slope (b)Intercept coefficient.

1.5.2 The Host galaxy subtracted AGN luminosity

The AGN fluxes at the time of our monitoring can be determined by subtracting the host galaxy fluxes from the total fluxes. During our monitoring campaign, the total B fluxes lie in the range between 5.81-8.39 mJy with a mean of 7.02 ± 0.11 mJy. The total V fluxes lie in the range between 8.17-10.38 mJy with a mean of 9.27 ± 0.11 mJy. The host galaxy subtracted average AGN fluxes are 4.69 ± 0.30 mJy in B and 4.54 ± 0.38 in V.

The interpolated rest frame 5100Å flux is $F_{5100\text{Å}} = 4.57 \pm 0.36$ mJy assuming a power law SED $F_\nu \propto \nu^\alpha$. The error was determined by interpolating between the ranges of AGN fluxes $\pm\sigma$ in both filters respectively.

At the distance of 145.0 Mpc (Bentz et al. 2009), we have obtained the monochromatic AGN luminosity $\lambda L_{\lambda(AGN)}(5100\text{Å}) = 6.73 \pm 0.53 \times 10^{43}$ erg/s with an uncertainty of 8%. The AGN luminosity during our campaign is about 54% smaller than the mean value of $12.40 \pm 2.6 \times 10^{43}$ erg/s derived by Bentz et al. (2009) from the host galaxy modeling using the high-resolution HST images and with parameters of the host galaxy determined by the GALFIT program (Peng et al. 2002). The difference is mainly due to the different value for the host galaxy contribution. They determine a host galaxy flux of $0.78 \times 10^{-15}\ ergs^{-1}cm^{-2}\text{Å}^{-1}$, which after the correction for extinction gives 1.98 mJy. This last value is about 40% smaller than our host galaxy flux in V.

Fig (1.9) shows the B versus V fluxes measured using an aperture of 7.5". The dotted blue lines represent the range of the AGN flux in both filters. We also show the results for the host galaxy fluxes obtained by Bentz et al. (2009) and Sakata et al. (2010).

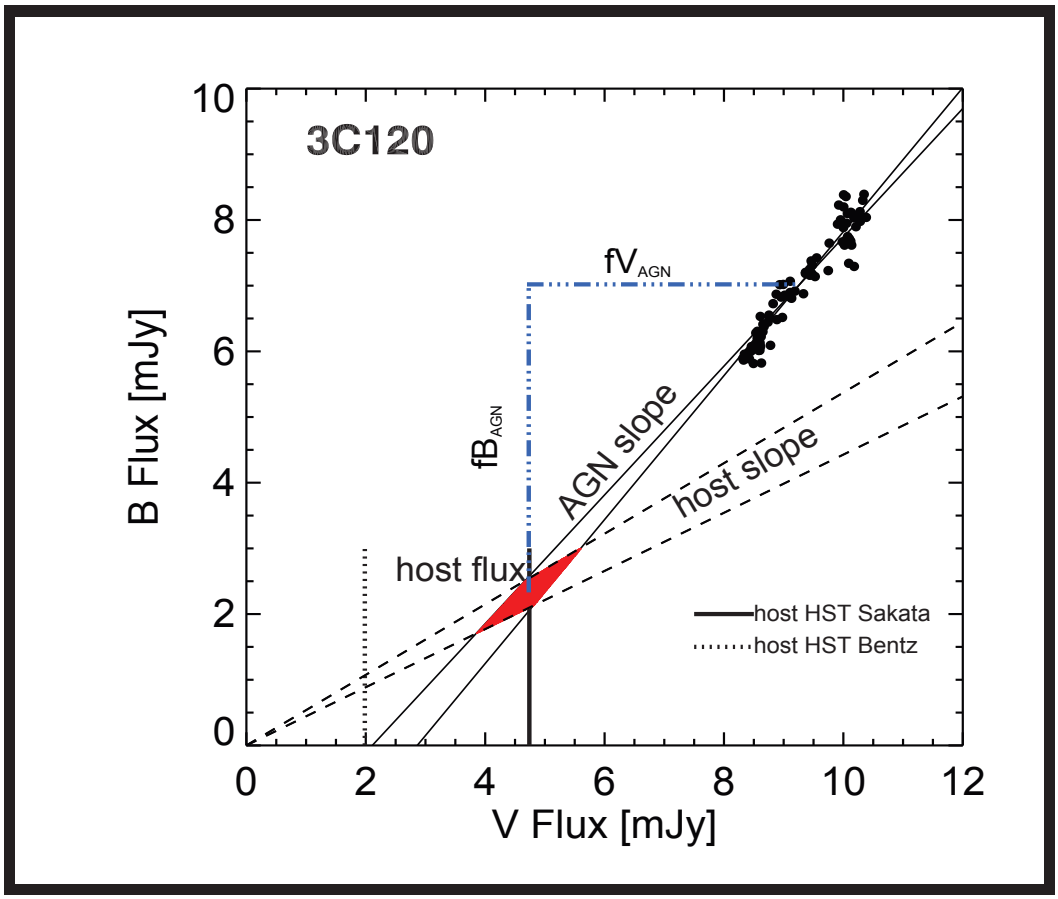

Figure 1.9 . B versus V fluxes of 3C120, measured with 7.5" aperture.

To understand the difference between our results and those Bentz et al. (2009), i.e. between the results obtained by the FVG and GALFIT method, we perform the following tests. 1) We change the host galaxy range consider the possible errors in the slopes but not similar values were found. 2) we calculated the slope of AGN using 5 different linear regression methods. Only the OLS(X/Y) method results in a slope of $\Gamma_{BV} = 1.04 \pm 0.07$. However, this slope is too large to intersect range of slopes of the host galaxy fluxes.

Finally we have plotted the FVG diagram with the data not corrected for extinction to test for possible systematic errors introduced by this correction. We also plot the data for the different apertures. However, the slope of the AGN spectrum remains steep. We therefore conclude that the different results cannot be attributed to errors in only the FVG method. A possible explanation for the difference is that a fraction of the bulge of a nuclear starburst in 3C120 is not resolved in the HST image and thus do not get modelled with GALFIT.

1.5.3 Nuclear color and absolute magnitude

In the section 1.4.2 we obtained the best-fit regression line from the flux-to-flux diagram using the optimal aperture. The results allow us to corroborate the steep AGN slope of 3C120 and to deduce immediately the optical nuclear color of the AGN to be $(B-V)_{nucleus} = -0.008 \pm 0.04$. This results is in good agreement with the intrinsic colors of the variable component in Seyferts galaxies determined by Winkler et al. (1992).

We have determined the B and V absolute magnitude of the nucleus following the method described by Véron-Cetty & Véron (2010), where the absolute magnitude is given by:

$$M = m + 5 - 5\log D - k + \Delta m(z) \tag{4}$$

m_B is the B mean apparent magnitude of the nucleus, D is the luminosity distance introduced by Riess et al. (2004) and defined as:

$$D = c/H_0 \times (1+z) \int_0^z [(1+z)^3 \times \Omega_M + \Omega_\Lambda] \tag{5}$$

and k is the magnitude correction for an object at redshift z and defined as:

$$k = -2.5 \log(1+z)^{1-\alpha} \tag{6}$$

Finally, $\Delta m(z)$ is a constant representing a correction to the k value and is given by Véron-Cetty & Véron (2010). Véron-Cetty & Véron (2010) used a spectral index $\alpha = 0.3$ as determined by Francis et al. (1991) from fitting the continuum between the $B - UV$ range for several AGN including some reddened ones. The inclusion of reddened AGNs was noted by Winkler (1997), and to correct for this we use a spectral index of $\alpha = 0.7$ which corresponds to the $U - B = 1.1$ determined by Winkler (1997). Using values for a flat cosmology with $H_0 = 71\ km^{-1}s^{-1}Mpc^{-1}$, $q = 0$, $\Omega_M = 0.29$ and $\Omega_\Lambda = 0.71$ yields a final value for the absolute magnitude of the nucleus of $M_B = -20.94 \pm 0.1$.

1.6 Ark120

Ark120 (redshift $z = 0.0327$) is a Seyfert 1 galaxy known to show strong flux variations in the continuum and highly variable emission lines (Peterson et al. (1989)). Photometric studies using broad band filters have shown significant optical variations during long term monitoring, with amplitude in the B-Band about 2.1 mag and short term outbursts of about 1.4 mag (Miller 1979). Later studied found smaller amplitude variations in the B-Band of 0.4 mag (Winkler et al. 1992) and about 0.8 mag (Doroshenko et al. 2008).

Microvariability has also been observed on timescales of 1.66 hr (Carini et al. 2003). However, the previous observations do not allow to discriminate between different models of AGN variability. This results are only an exception with respect to a larger sample of Seyfert galaxies but also have shown that Ark120 has a extended host galaxy contribution.

1.6.1 The host galaxy flux determination

Fig (1.10) shows the B versus V flux diagram for the different apertures used. All data were corrected for Galactic foreground extinction using the values determined by Schlegel et al. (1998). The solid lines represent the best-fit regression model and yield a range for the AGN slope in each aperture. The dotted lines represent the range of host slopes obtained by Sakata et al. (2010) and the intersection between these lines and the range for the AGN slope yields the host flux in both bands (differently colored shaded areas represent the results for the different apertures). The black, red and blue points correspond to an aperture diameter of 5", 7.5", and 15" respectively. The open squares represent the extremes in fluxes obtained by Winkler et al. (1992) using a 20" aperture and adopting $E_{B-V} = 0.1$. The dotted lines through these points correspond to the AGN slope.

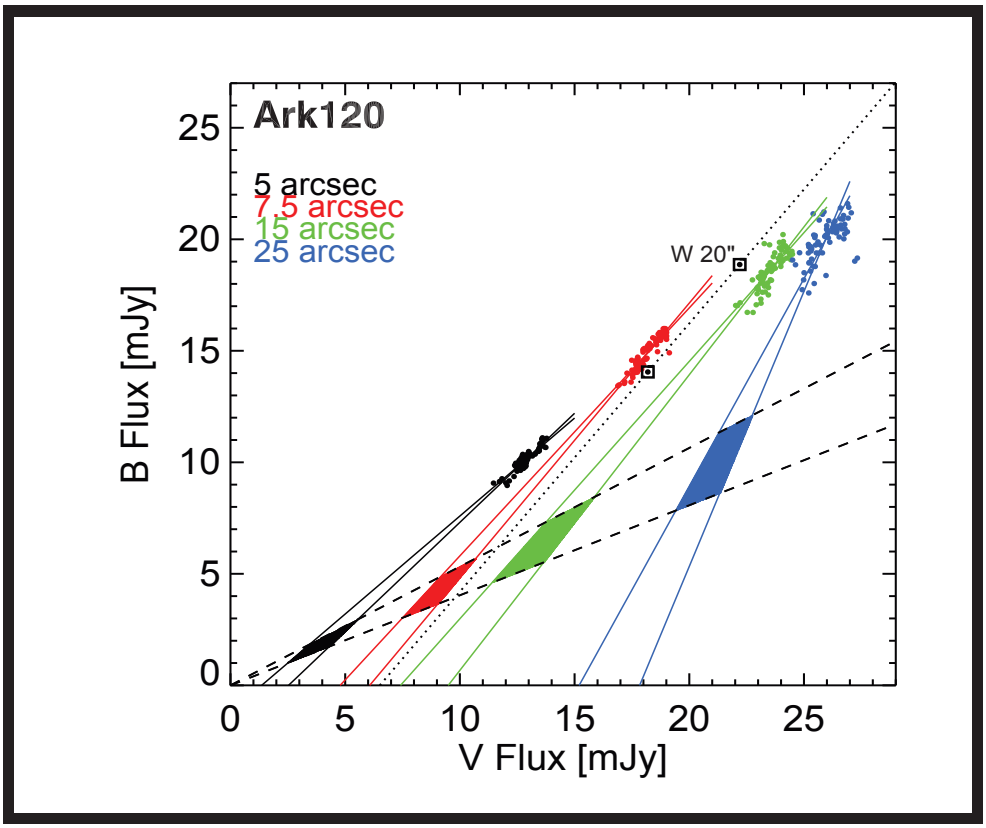

Figure 1.10 . B versus V fluxes of Ark120, measured with different apertures.

Again the optimal aperture was 7.5" and together with the best fit regression line yields a linear gradient of $\Gamma_{BV} = 1.19 \pm 0.06$, consistent with $\Gamma_{BV} = 1.20 \pm 0.10$ determined by Winkler et al. (1992) and $\Gamma_{BV} = 1.22 \pm 0.02$ determined by Doroshenko et al. (2008) correcting their data by extinction. Averaging over the intersection area between the AGN and the host galaxy slopes, we obtain a mean host galaxy flux of 4.26 ± 0.59 mJy in B and 9.02 ± 0.62 mJy in V, which represent a contribution of about 50% in V and about 28% in B band with respect to the total flux. These results are consistent with the values $fB \approx 4.5mJy$ and $fB \approx 9mJy$ obtained by Doroshenko et al. (2008) from a FVG analysis of UBVRI data. The results obtained for each aperture and linear regression analysis are listed in Tab (1.4) and Tab (1.5) respectively.

Table 1.4. Photometry results of Ark120 for each aperture

Name	Date	aperture [arcsec]	B [mag]	σ_B	V [mag]	σ_V	$fB_{total}[mJy]$	$fV_{total}[mJy]$
$Ark120$	$October.2009 - March.2010$	5	$13.96 - 14.19$	$0.026 - 0.028$	$13.61 - 13.81$	$0.012 - 0.017$	10.10 ± 0.19	12.85 ± 0.21
		7.5	$13.56 - 13.76$	$0.024 - 0.022$	$13.26 - 13.39$	$0.029 - 0.018$	15.09 ± 0.73	18.18 ± 0.57
		15	$13.31 - 13.52$	$0.065 - 0.063$	$12.99 - 13.10$	$0.036 - 0.017$	18.56 ± 0.94	23.49 ± 0.54
		25	$13.24 - 13.46$	$0.082 - 0.110$	$12.87 - 12.99$	$0.040 - 0.037$	19.96 ± 2.24	25.93 ± 1.25

Note. — All data were corrected for galactic foreground extinction using the values determined by Schlegel et al. (1998). fB_{total} and fV_{total} refer to the mean of the total flux ranges during our monitoring campaigns.

Table 1.5. Linear regression results for Ark120

Name	aperture [arcsec]	method	a^a	σ_a	b^b	σ_b
*Ark*120	5	$OLS(X/Y)$	0.93	0.05	−1.84	0.64
	5	$OLS(Y/X)$	1.10	0.06	−4.03	0.79
	5	OLS Bisector	1.01	0.05	−2.89	0.68
	5	*Orthogonal Regression*	1.01	0.06	−2.90	0.74
	5	RMA	1.01	0.05	−2.89	0.68
	7.5	$OLS(X/Y)$	1.19	0.06	−6.39	1.08
	7.5	$OLS(Y/X)$	1.36	0.06	−9.81	0.84
	7.5	OLS Bisector	1.26	0.06	−8.03	0.85
	7.5	*Orthogonal Regression*	1.28	0.05	−8.44	0.89
	7.5	RMA	1.26	0.05	−8.04	0.85
	15	$OLS(X/Y)$	1.24	0.09	−10.57	2.01
	15	$OLS(Y/X)$	1.82	0.17	−24.17	4.02
	15	OLS Bisector	1.49	0.11	−16.48	2.47
	15	*Orthogonal Regression*	1.63	0.15	−19.66	3.55
	15	RMA	1.50	0.11	−16.72	2.56
	25	$OLS(X/Y)$	0.85	0.15	−2.02.23	3.92
	25	$OLS(Y/X)$	2.16	0.30	−36.14	7.85
	25	OLS Bisector	1.31	0.11	−14.12	2.84
	25	*Orthogonal Regression*	1.61	0.20	−21.69	5.28
	25	RMA	1.35	0.12	−15.15	3.010

Note. — Linear regression results for OLS(X/Y), OLS(Y/X), OLS Bisector, Orthogonal Regression and the Reduced Major Axis methods. (a)Slope (b)Intercept coefficient.

1.6.2 The Host galaxy subtracted AGN luminosity

The AGN fluxes at the time of our monitoring can be determined by subtracting the host galaxy fluxes from the total fluxes. The host galaxy subtracted AGN fluxes range between 10.82 ± 0.94 in B and 9.14 ± 0.84 in V. Extrapolating and assuming a distance of 141.8 *Mpc* (Bentz et al. 2009) give a rest-frame 5100Å flux of $F_{5100\text{Å}} = 9.41 \pm 0.86$ mJy. We determined the AGN luminosity to be $\lambda L_{\lambda(AGN)}(5100\text{Å}) = 13.27 \pm 1.21 \times 10^{43}$ erg/s with an uncertainty of 10%.

Bentz et al. (2009) determined an AGN luminosity of $\lambda L_{\lambda(AGN)}(5100\text{Å}) = 8.47 \pm 0.81 \times 10^{43}$ erg/s. We performed some tests to understand the difference between these results. Fig (1.11) shows the B versus V fluxes for the 7.5" aperture. The dotted blue lines represent the range of the AGN flux in both filters and also plotted are the result for the host galaxy flux obtained by Bentz et al. (2009), using a slit area of 5"×7.6". Our aperture is only 16% larger, and the V band results give consistent results for the flux at $F550M \approx 10mJy$. We then calculated the total observed fluxes at rest-frame 5100Å to be $F_{5100\text{Å}} = 13.4 \times 10^{-15}\ ergs^{-1}cm^{-2}\text{Å}^{-1}$ during our campaign. Peterson et al. (1998a) found the total fluxes to range between $7.82 - 10.37 \times 10^{-15}\ ergs^{-1}cm^{-2}\text{Å}^{-1}$ during his eight years of monitoring the source.

From the comparison we conclude that the difference in results is due to the fact that the nucleus of Ark120 was brighter by about 50% during our monitoring in 2011.

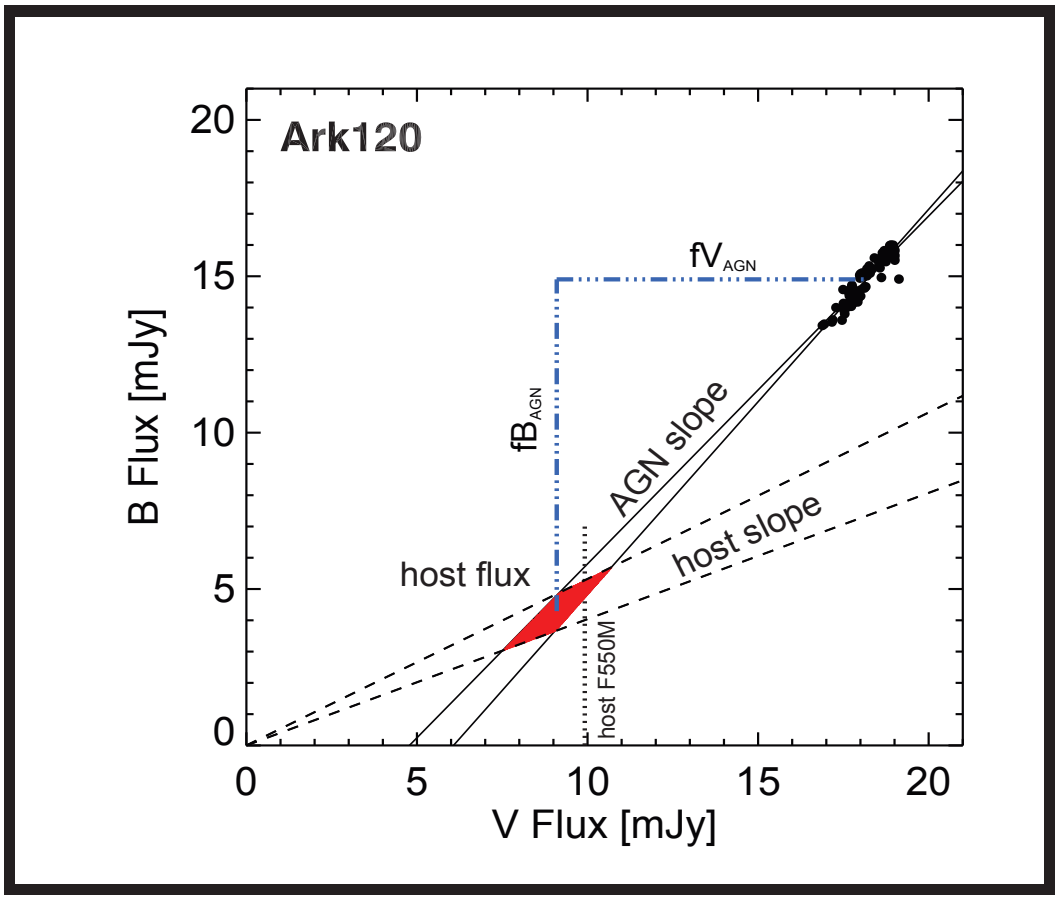

Figure 1.11 . B versus V fluxes of Ark120, measured with 7.5".

1.6.3 Nuclear color and absolute magnitude

Analogous to 3C120 we subtract the host galaxy flux identified using the FVG method to determined a B-V color index of $(B-V)_{nucleus} = -0.07 \pm 0.06$ for the variable component. Once again this result is in good agreement with the intrinsic colors of the variable component for Seyferts galaxies determined by Winkler et al. (1992). The absolute magnitude of the nucleus was determined to be $M_B = -21.79 \pm 0.1$.

1.7 Discussion and Conclusions

We have presented five months of new photometric B and V band data for the Seyferts 1 galaxies 3C120 and Ark120.

For 3C120 the observed light curve (host+nucleus) shows a variation amplitude of about 0.4 mag between MJD 55169 and 55209. Once the contribution of the host galaxy is subtracted, the amplitude of the variability for the optical continuum emission is about 0.7 mag (see Fig 1.13). The rapid fading of the nucleus is a notable feature in these time observations of 3C120, considering that the amplitude of variations observed in previous year-long studies (0.4 mag, Winkler et al. 1997; 1.5 mag, Sakata et al. 2010).

The total light curve of Ark120 shows on average a variation amplitude of about 0.25 mag in 30 days. After subtracting the host galaxy component, the variability amplitude of the optical continuum emission is about 0.32 mag (see Fig 1.17). The source shows rapid, 20 to 60-day timescale variability between MJD 55141 and 55161 when the source increased by 0.2 mag and between MJD 55201 and 55266 when the sources faded by about 0.35 mag. This are significant signs of variability in a very short timescale. Doroshenko et al. (2008) observed an increase in nuclear brightness of 1 mag between MJD 52500 and 53500, when the B magnitude reached 13.6 mag.

In both cases we observed that despite of high level of variability, the color of the nucleus remains approximately constant during the complete monitoring observations. Our results show good agreement with respect to the intrinsic colors of the variable component for Seyferts 1 galaxies (Winkler et al. 1992) and this confirms that the variable component for 3C120 and Ark120 has a blue constant color dominates over the reddened non-variable component and which is the expected behavior for the nuclear continuum color in Seyferts 1 galaxies.

Has been shown that by means of the flux variation gradient (FVG) method and the previously defined host galaxy color range, is possible to find the host galaxy subtracted AGN luminosity with uncertainties of 8% and 12% for 3C120 and Ark120, respectively (see Tab 1.6). The small uncertainties compared to previous results is due to the 50% smaller uncertainties in the host galaxy flux contribution.

Table 1.6. Host-subtracted results for 3C120 and Ark120

Name	$fB_{total}[mJy]$	$fB_{host}[mJy]$	$fB_{AGN}[mJy]$	$fV_{total}[mJy]$	$fV_{host}[mJy]$	$fV_{AGN}[mJy]$	$f_{AGN}((1+z)5100\text{Å}[mJy]$	$\lambda L_{\lambda,AGN}(5100\text{Å})10^{43} ergs^{-1}$
$3C120$	7.02 ± 0.11	2.33 ± 0.28	4.69 ± 0.30	9.27 ± 0.10	4.73 ± 0.36	4.54 ± 0.37	4.57 ± 0.36	6.73 ± 0.53
$Ark120$	15.09 ± 0.73	4.26 ± 0.59	10.82 ± 0.94	18.18 ± 0.57	9.02 ± 0.62	9.16 ± 0.84	9.41 ± 0.86	13.27 ± 1.21

Note. — All data were corrected for galactic foreground extinction using the values determined by Schlegel et al. (1998). fB_{total} and fV_{total} refer to the mean of the total flux ranges during our monitoring campaigns. $fB_{AGN} = fB_{total} - fB_{host}$ and $fV_{AGN} = fV_{total} - fV_{host}$, with uncertainty range $\sigma_{AGN} = (\sigma^2_{total} - \sigma^2_{host})^{0.5}$.

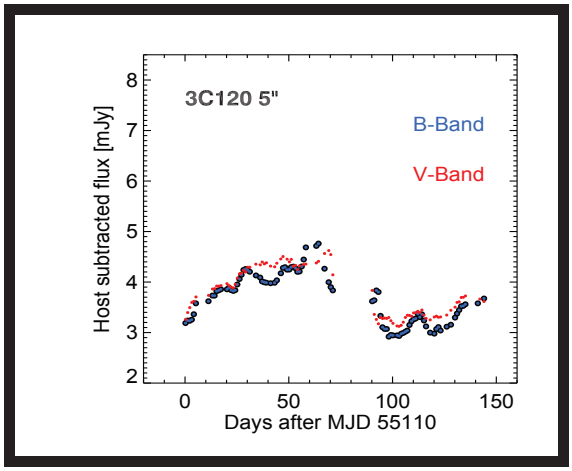

Figure 1.12 Light curve of the nucleus using the 5" aperture.

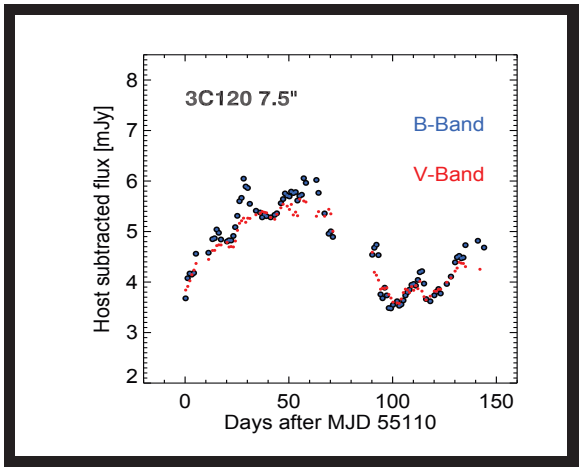

Figure 1.13 Light curve of the nucleus using the 7.5" aperture.

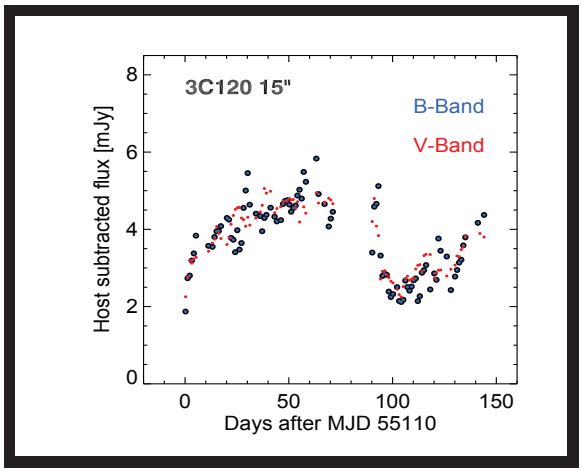

Figure 1.14 Light curve of the nucleus using the 15" aperture.

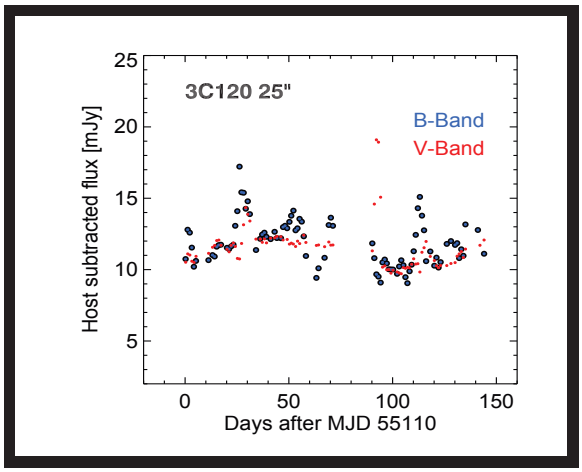

Figure 1.15 Light curve of the nucleus using the 25" aperture.

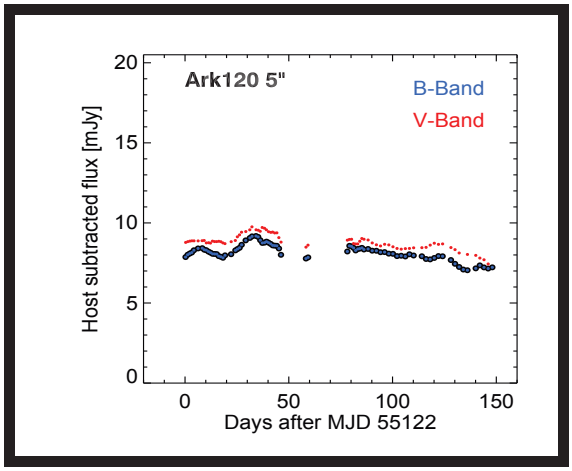

Figure 1.16 Light curve of the nucleus using the 5" aperture.

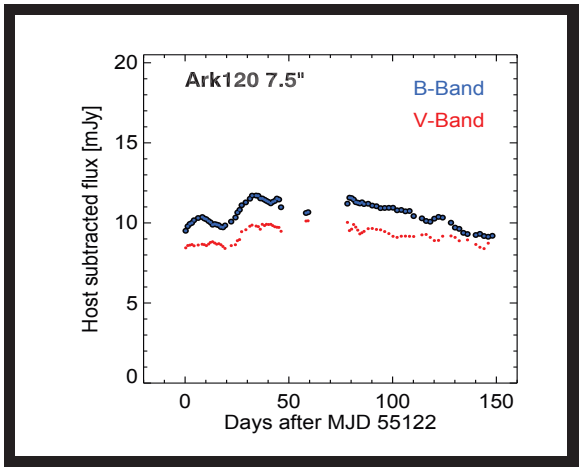

Figure 1.17 Light curve of the nucleus using the 7.5" aperture.

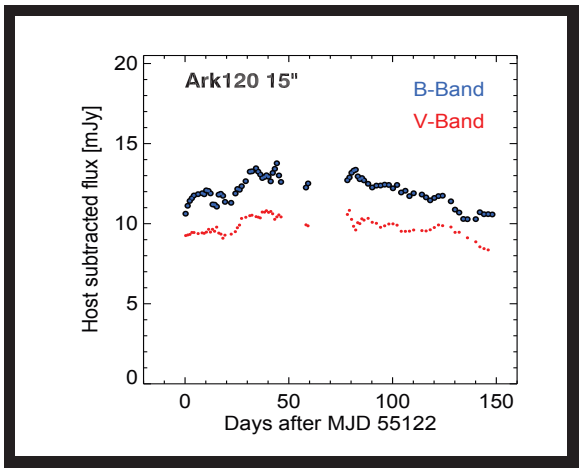

Figure 1.18 Light curve of the nucleus using the 15" aperture.

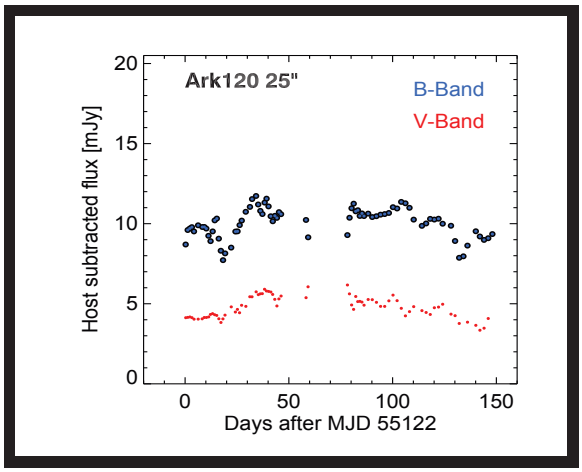

Figure 1.19 Light curve of the nucleus using the 25" aperture.

Chapter 2

Narrow-band echo mapping of Active galactic nuclei

2.1 Introduction

The method of reverberation mapping was proposed by Blandford (1982). This method has been widely used in the present in the study of the physical properties of the broad line region (BLR) in active galactic nuclei (AGN). This method with further improvements (Horne 2001; Peterson 2001) has allowed for the determination of the size, gas kinematics and distribution within the BLR. At present, is well known that the luminosity variations that occur in the variable continuum emitting region produce a variation in the broad emission lines, which arise near the hot accretion disk.

Because the BLR is close to the accretion disk we can assume directly that the gas motions in the BLR are remarkably influenced by the gravitational potential of the central super-massive black hole. As a result the lines are broadened by Doppler velocities of about 10^{3-4} kms^{-1} for UV and optical spectra respectively.

The lines respond to the continuum variations occur with a small time delay (usually called "echo") related to the time needed for the light to travel between the accretion disk and the BLR. Because of the high density the gas will react instantaneously to the change in illumination and the time delay is only due to the distance of the BLR from the accretion disk. Therefore this lag, depends directly of the light-travel time across the BLR geometry. Multiplying the time delay by the speed of light, we obtain an approximate size of the BLR, which if combined with the velocity dispersion of gas measured from the Doppler-broadened emission-line width gives the mass of the central black hole (Peterson et al. 2004, Kaspi et al. 2000, Vestergaard 2002).

While determining the BLR size allows us to obtain the mass of central supermassive black hole, we can also use this measure to determine cosmic distances to AGN using the relationship $R_{BLR} \propto L^{\alpha}$. This relationship between the BLR size and absolute luminosity for AGNs is currently used to determine distances to AGN.

To date only in a handful of relatively nearby type 1 AGN has the reverberation mapping been successful in determining the time lag (Peterson et al. 2004), while that due to time dilation effects, the delay time can not be measured for objects at high redshifts and we would need very long observation programs (Kaspi et al 2007). The size of the BLR ranges from a few light days to hundreds of light days. Therefore is necessary to perform observational monitoring periods, ranging from months to years in order to have sufficient measurements to distinguish and measure the "echoes". Most observational campaigns have monitored the sources by taking spectra over these timescales, which demands large amounts of telescope time.

Here we propose to use a method that is less demanding telescope time but gives consistent results. This method is called photometric reverberation echo

mapping and employs a wide bandpass to trace the AGN continuum and suitable narrow-bands to trace the echo of the BLR lines. In this study we establish the feasibility and complete application of this method for the determination of the BLR size and the mass of the black hole in a large sample of AGNs, and which also provides an opportunity to determine the cosmological distances to quasars.

In section 2.2 we explain how the data were obtained including observations, data reduction, description about the sample and the light curves obtained. In section 2.3 we review the method of reverberation mapping and implications in this work. In section 2.4, 2.5 and 2.6 we perform a time series analysis of the light curves for the different AGN under study:3C120, Ark120 and PG0003+199. All these sources have known BLR sizes in the literature. In section 2.7 we discuss our results and preliminary conclusions.

2.2 Sample, observations and data reductions

Photometric monitoring campaigns was conducted between August 2009 and March 2010 using the robotic 15 cm VYSOS6 telescope of the Universitätstternwarte Bochum installed at the Cerro Murphy Observatory in the Chilean Atacama desert. Details about VYSOS6 telescope are presented in section 1.2 (of chapter 1). Light curves were obtained in the B-band (Johnson band pass $= 4250 \pm 500$Å), V-band (Johnson band pass $= 5500 \pm 500$Å), redshifted $H\alpha$ (NB$= 6721 \pm 30$Å) and $H\beta$ (NB$= 5007 \pm 30$Å) lines.

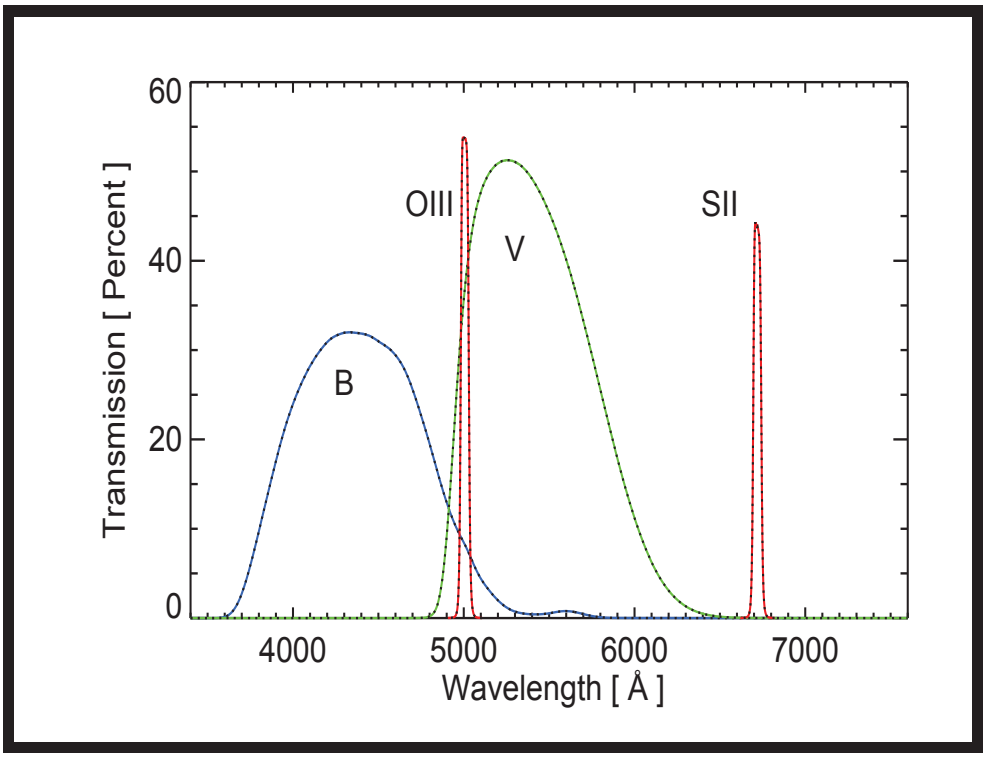

Figure 2.1 . Effective transmission of the filters convolved with the quantum efficiency of the ALTA U16M CCD camera.

Observations were performed with a mean sampling of 2-3 days. The effective transmission for each filter can be seen on Fig (2.1). The positions, galactic extincion (derived from Schlegel et al. 1998) and the distances of the AGN observed are listed in Tab (2.1). Additionally, one spectrum for each object was obtained using the CAFOS instrument at the 2.2 m telescope on Calar Alto, Spain, using a slit width of 1.54". The reduction of the spectra was performed using standard IRAF procedures to reduce spectroscopy data from CAFOS instrument[1]. The reduced spectra are presented in Fig (2.2).

[1]IRAF procedure to reduce SPSS Calar Alto observations, prepared by: J.M. Carrasco, G. Altavilla. DPAC, Data Processing Analysis Consortium and reduced by Michael Ramolla (AIRUB).

Table 2.1. Source parameters

Name	other name	α (2000)	δ (2000)]	z	D_L	$A_B{}^{(1)}$	$A_V{}^{(1)}$
					(Mpc)	(mag)	(mag)
PG0003+199	Mrk 335	00 06 19.521	+20 12 10.490	0.02579	112.6	0.153	0.118
Ark120	Mrk 1095	05 16 11.421	-00 08 59.380	0.03271	141.8	0.554	0.426
3C120	Mrk 1506	04 33 11.095	+05 21 15.620	0.03301	145.0	1.283	0.986

Note. — (1)Values used to correct for galactic extinction in B and V band from Schlegel et al. 1998.

2.3 Review of the reverberation mapping method

Our current understanding of the structure of the central engine of active galaxies involves the accretion of gas from an accretion disk onto a super-massive black hole (SMBH). The inner part of the accretion disk, with a typical size of $10^{13-10^{14}}$ cm, generates the variable continuum emission and which is highly variable on different scales of time. Orbiting around of these SMBH/accretion disk system is the BLR, a large amount of gas clouds ionized by the radiation from the accretion disk (about 10-100 light days). Observationally this region is identified through its broadened emission lines.

The reverberation mapping method was first proposed by Blandford & Mckee (1982). Variations in the broad lines will show a delay compared to the continuum variability depending on the distance of the BLR and the accretion disk.

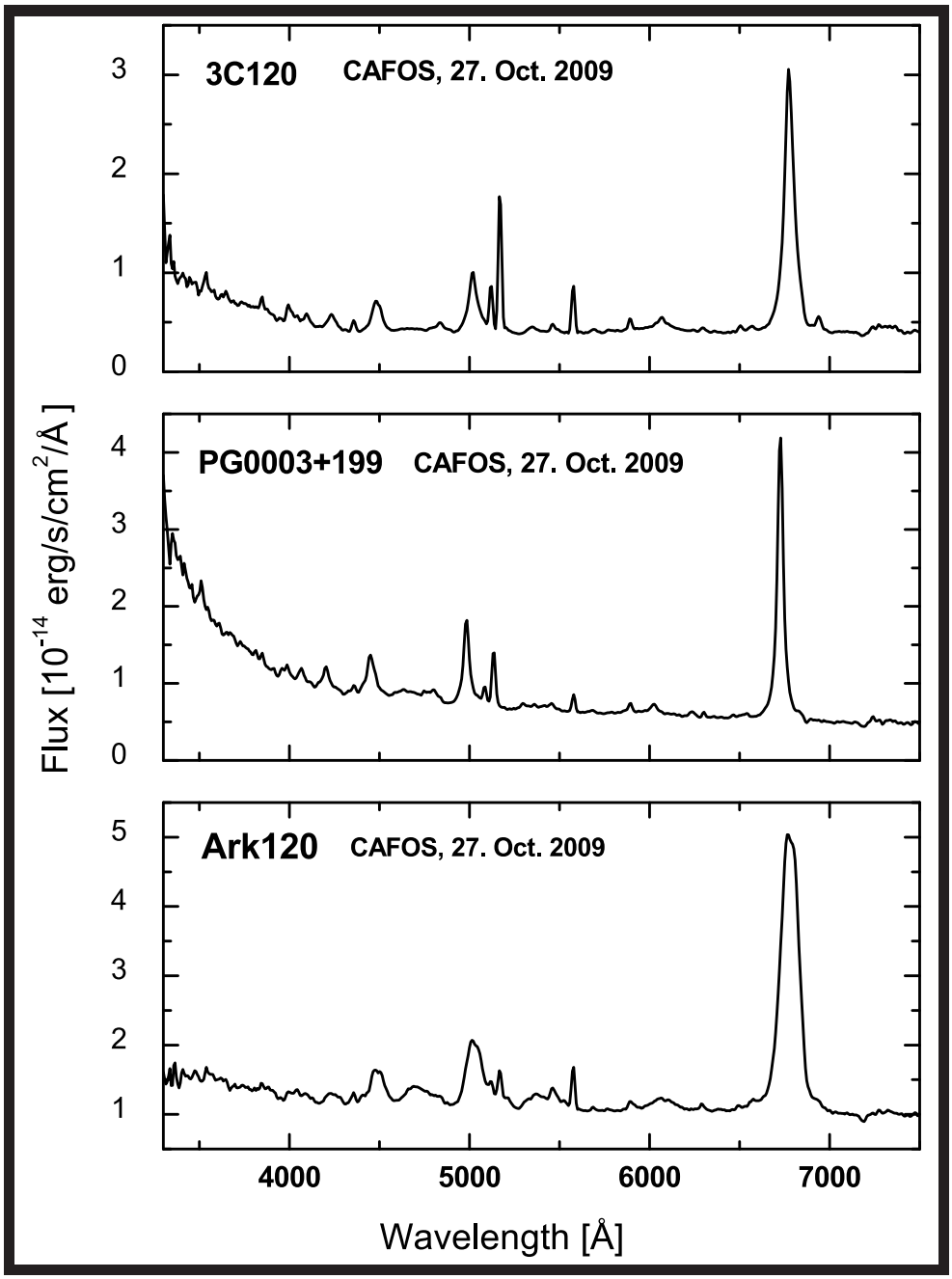

Figure 2.2 .Observed spectrum of 3C120, PG0003+199 and Ark120 respectively.

The time delay of the echo can be determined by cross-correlation techniques on the light curves measured for the emission line and the continuum region. Thus, is possible to deduce the size of the BLR orbit as:

$$R_{BLR} = \tau \cdot c \tag{2.1}$$

where c is the speed of the light and τ is the mean time lag. The mean of the time lag can be determined using the discrete correlation function (DCF hereafter) defined by Edelson & Krolik (1998) as:

$$DCF(\tau) = \left\langle \frac{(a_i - \overline{a})(b_i - \overline{b})}{\sqrt{(\sigma_a^2 - e_a^2)(\sigma_b^2 - e_b^2)}} \right\rangle \tag{2.2}$$

in general terms, the pairs (a_i, b_j) correspond to each discrete sets of data associated the pairwise lag $\Delta t_{ij} = t_j - ti$, as is mentioned in the analysis of Edelson & Krolik (1998). The averaging of the DCF is taken for all pairs of data points i, j for which $\tau - \Delta\tau/2 \leq t_i - t_j < \tau + \Delta\tau/2$. In subsequent studies the terms e_a and e_b were considered to be zero, due to the problems with the interpretation (M.Bonne & G. Spears 2004). This was also adopted in our calculations.

From a single epoch spectrum we can measure the orbital velocity of the clouds of the BLR by calculating the line dispersion (from the width of the emission line) defined as:

$$\sigma_{line}^2 = \frac{\int \lambda^2 F(\lambda) d\lambda}{\int F(\lambda) d\lambda} - \left[\frac{\int \lambda F(\lambda) d\lambda}{\int F(\lambda) d\lambda} \right]^2 \tag{2.3}$$

where $F(\lambda)$ is the line flux at wavelenght λ.

Combining the results for the time delay and the orbital velocity and using Kepler's laws we can determine the mass of the black hole using:

$$M_{BH} = f\frac{c \cdot \tau \cdot V^2}{G} \tag{2.4}$$

where $f \approx 1.0$ is a factor that depends on the geometry (angle of inclination) and kinematics of the BLR.

2.4 Results for 3C120

Fig (2.3) depicts the light curves of 3C120. The B-band shows a steeply increase reaching a maximum in early November 2009. Afterwards the flux decreased until mid-November 2009 before increasing again and reaching a second maximum during the first days on December 2009. The flux was very similar after the data gaps between mid-December 2009. After the lost data from mid-December and early January, we see that the flux has increased very little after the previous minimum. By mid January the flux decreases more rapidly.

Between the end of January and early February, the variability is more regular and the flux increases again to reach a third maximum at the end of February 2010. In contrast to the steep B band flux increase, the NB flux increase is stretched until December 2009 to its first maximum. The sharp decrease in flux in the B band, after the second peak in late December 2009, is reflected in the NB in early January 2010. Thus as a first approximation the delay time is 28 days.

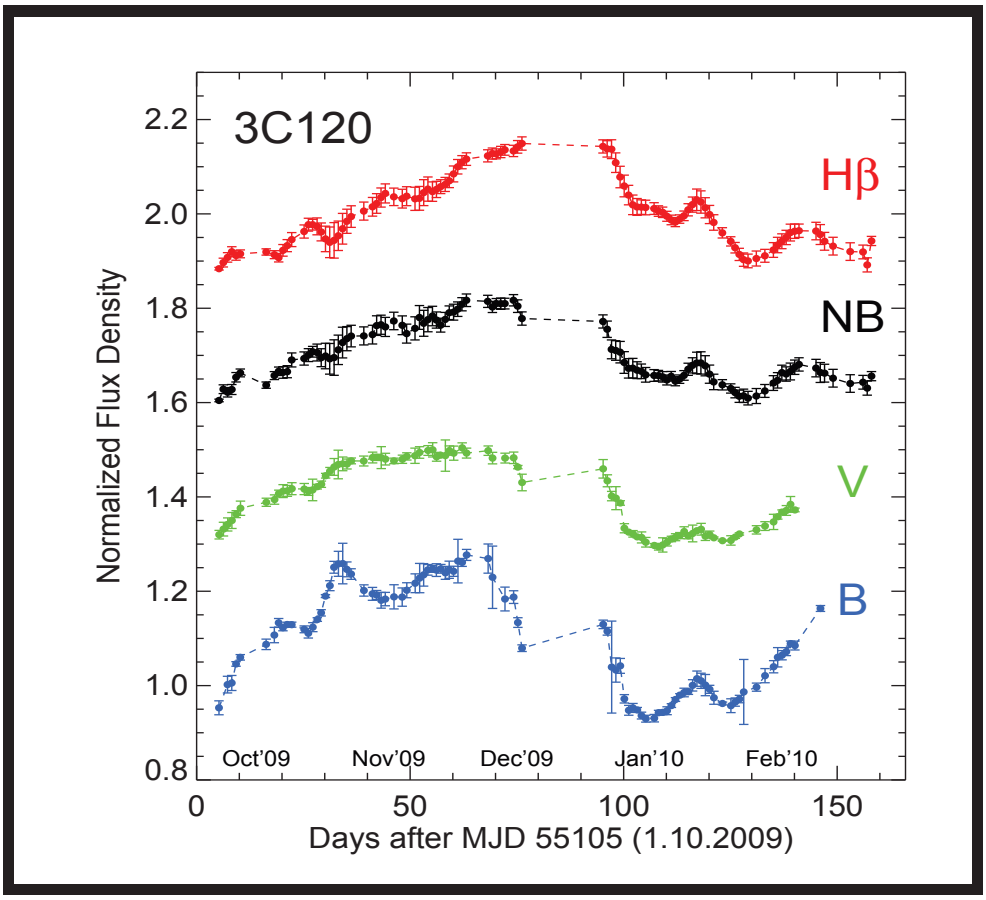

Figure 2.3 .Observed light curves for 3C120 between Oct. 2009 and March 2010. The light curve is computed by subtracting a scaled V curve from the NB curve and re-normalized to mean = 1. The light curves were shifted by multiples of 0.1 for clarity. The data gap between the end of December 2009 and beginning of January 2010 is mostly due maintenance to the telescope.

The NB filter contains about 50% continuum emission and 50% $H\beta$ line emission, as shown in Figs. (2.1) and (2.2). In order to remove the continuum contribution, we computed a synthetic $H\beta$ light curve by subtracting a scaled the continuum component from the NB filter fluxes: $H\beta = NB - 0.5V$. We use the discrete correlation function to cross correlate the $H\beta$ and B-band light curves.

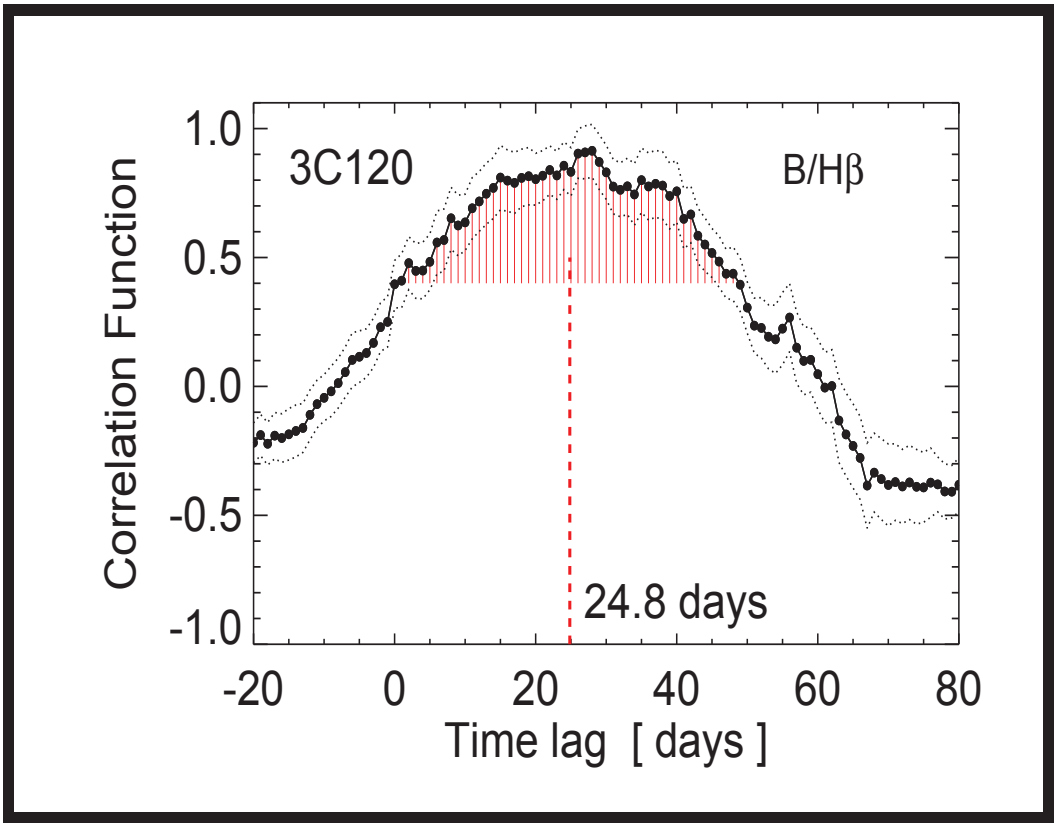

Figure 2.4 .Results of the cross correlations between B and $H\beta$ light curves. The dotted lines indicate the error range ($\pm\sigma$) around the cross correlation. The red area marks the range used to calculate the centroid of the lag, which is represented by the vertical red dashed line.

The cross correlation shows a major peak for a time delay of 24.8 days, as is defined by the centroid τ_{cent} in Fig (2.4).

To determine the uncertainty in the time delay we applied the flux randomization and random subset selection method (FR/RSS, Peterson et al. 1998b). From the observed light curves we create 2000 randomly selected subset light curves, each containing 63% of the original data points, and randomly altering the flux value of each data point consistent with its (normal-distributed) measurement error (Westhues, C. 2011).

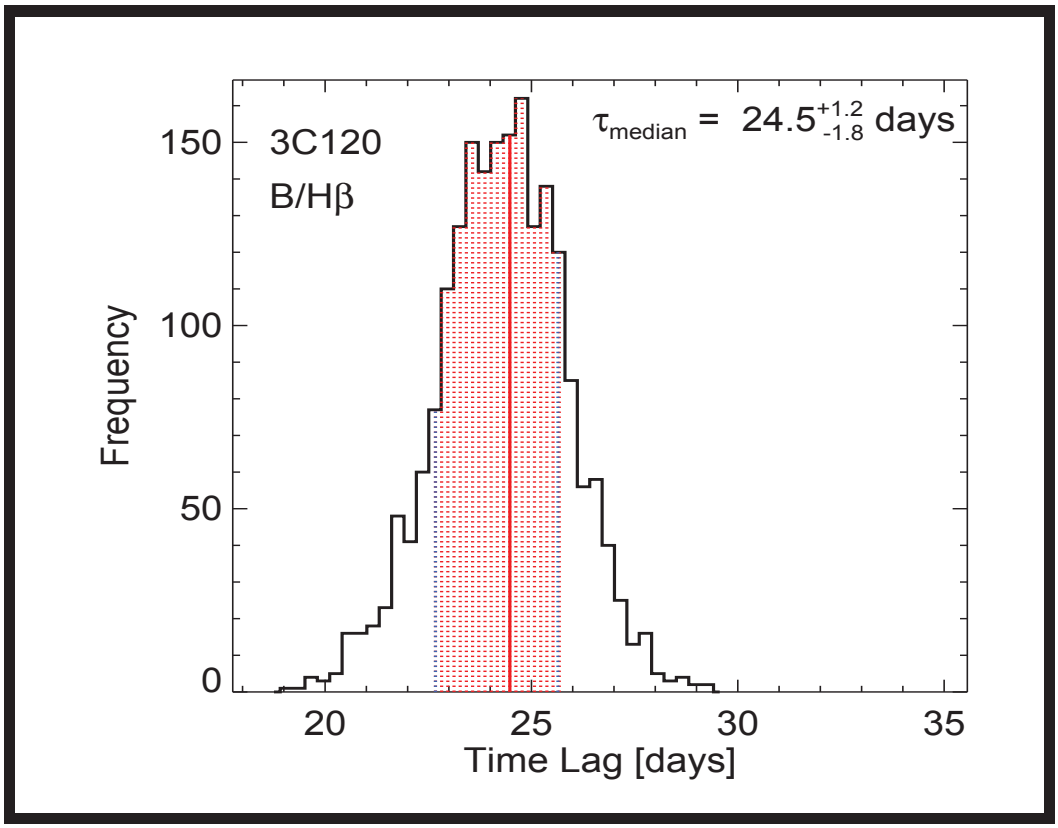

Figure 2.5 .Results of FR/RSS cross correlation for 3C120. The histogram shows the distribution of the centroid lag obtained by cross correlating 2000 flux randomized and randomly selected subset light curves. The red area marks the 68% confidence range used to calculate the errors of the centroid.

Discrete correlation function was applied to the 2000 pairs of subset light curves and the centroid τ_{cent} was calculated. Fig (2.5) shows a histogram with the distribution of the 2000 τ_{cent} values which yields a median lag $\tau_{cent} = 24.5^{+1.2}_{-1.8}$ days with an uncertainty of 6%. Correcting the mean lag time for the time dilation factor we obtain a rest frame lag $\tau_{rest-frame} = \frac{1}{1+z} \cdot \tau_{cent} = 23.7 \pm 1.45$ days. Previous investigation by Peterson et al. 1998a, 2004, through spectroscopic monitoring gives a value of $38.1^{21.3}_{-15.3}$ days with an uncertainty of 48%. We can see that our results have improved the previous measurement.

From the width of the emission line from our spectrum, we determined an intrinsic $H\beta$ line dispersion $\sigma_{line} = 1405.88 km/s$, this result is in agreement with the value obtained by Peterson et al. (2004). Using our rest frame time lag and assuming $f = 1.0$ we obtain a black hole mass of $M_{BH} = 9.15 \pm 1.2 \times 10^6 M_\odot$ consistent with $10.1 \pm 4.9 \times 10^6 M_\odot$ derived via spectroscopic reverberation mapping by Peterson et al. (2004).

2.5 Results for PG0003+199

Fig (2.6) depicts the light curves of PG0003+199. The AGN continuum as traced by the B-band increases gradually from August 2009 to peak around the end of September, followed by a steep drop of 20% at MJD 55118 (= 55045+73). The $H\alpha$ light curve shows a steep drop of about 10% with a delay time of about 20 days. The cross correlations shows a major peak at a time lag of 20.2 days as defined by the centroid τ_{cent} in Fig (2.7). Two smaller correlation peaks are observed with the time lags of 50 and 65 days. Both peaks are caused by the B-band through at beginning and middle of September 2009. From spectroscopic reverberation results Peterson et al. (2004) determined a time lag of less than 30 days. Hence, we do not further consider the two smaller peaks in this work. The distribution of the 2000 τ_{cent} values yields the median lag within the 68% confidence range. From this distribution we obtain a lag of $\tau_{cent} = 20.5^{+2.0}_{-2.8}$ days with uncertainty of about 12%, see Fig (2.8). Correcting for the time dilation factor yields a rest frame lag of $\tau_{rest-frame} = 20.0 \pm 2.35$ days. We did not find $H\alpha$ lags of PG0003+199 in the literature, but we can compare our result with that obtained for the $H\beta$ line using spectroscopic reverberation mapping. From spectroscopic reverberation an average rest frame time lag of 15.7 ± 3.7 day averaged over several epochs was obtained (Peterson et al. 2004, Bentz et al. 2009). This $H\beta$ lag is about 30% smaller than our $H\alpha$ lag of 20.0 days.

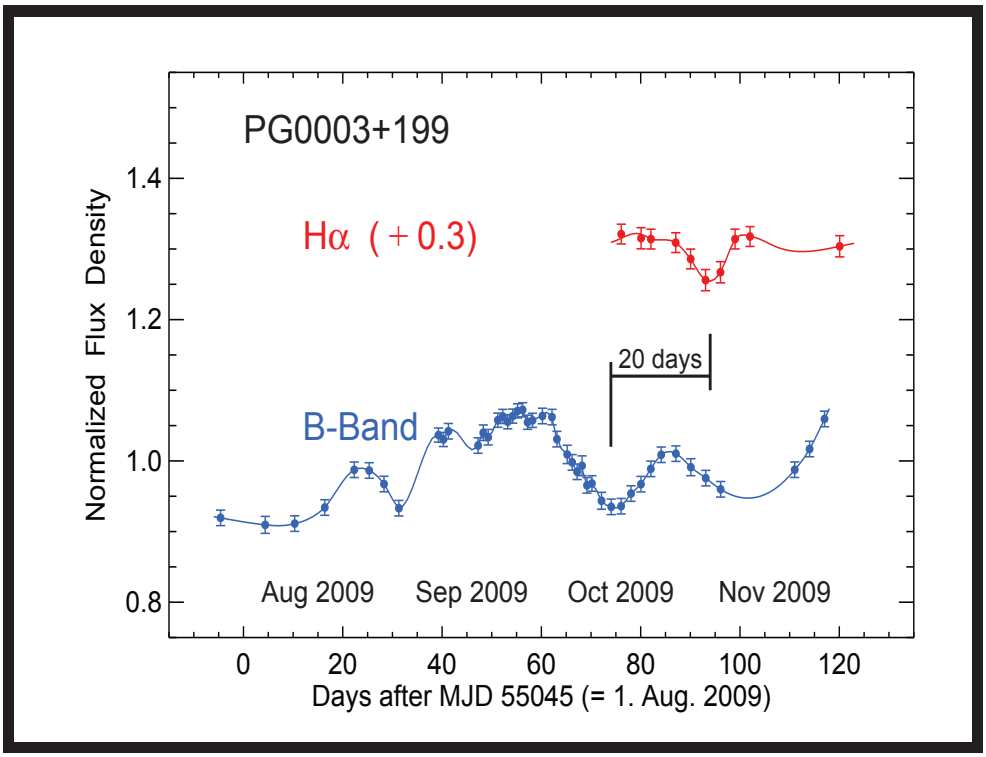

Figure 2.6 .Observed light curves of PG0003+199. The $H\alpha$ observations were started in October 2009 after recognizing the pronounced B-band variations.

A possible explanation is that the BLR size is smaller for higher excitation emission lines. Kaspi et al. (2000) found that the BLR $H\beta$ size is directly proportional to BLR $H\alpha$ size with a constant of proportionality 1.19 ± 0.23 using spectroscopic reverberation data from 17 PG quasars.

Kollatschny (2003a) provides evidence that the BLR in the Seyfert 1 galaxy Mrk 110 is stratified and the difference in time lags is 1.37. Recently the Lick AGN Monitoring Program of 11 low-luminosity AGN found an factor of 1.54 ± 0.4 (Bentz et al. 2009) with a similar uncertainty to that determined by Kaspi et al. (2000) In conclusion, it could be that the BLR is stratified and that the factor of proportionality depends on the luminosity of the AGN.

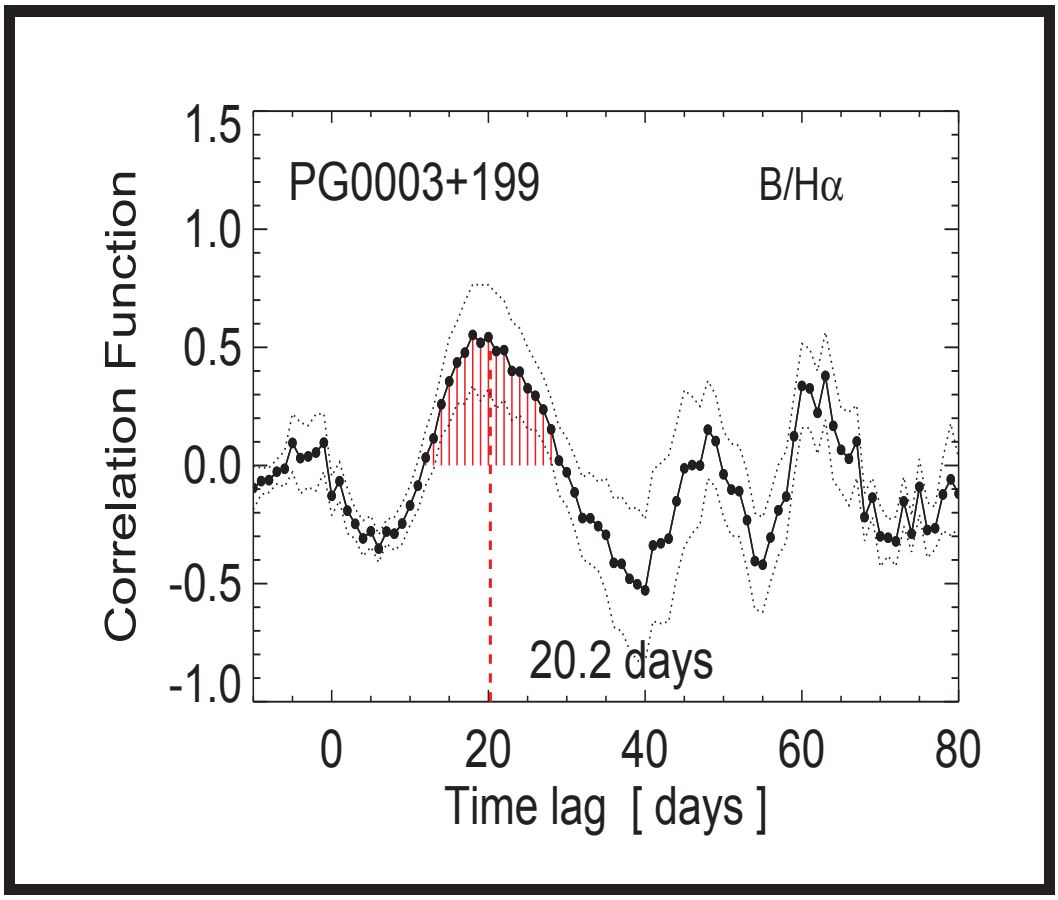

Figure 2.7 .Results of the cross correlations between the B and $H\alpha$ light curves. The dotted lines indicate the error range ($\pm\sigma$) around the cross correlation. The red area marks the range used to calculate the centroid of the lag, which is represented by the vertical red dashed line.

Considering that the luminosity of PG0003+199 is similar to that of Mrk 110, we use the factor determined by Kollatschny (2003a). Thus, the $H\beta$ lag of PG0003+199 translates into an $H\alpha$ lag of $15.7 \times 1.37 = 21.5$ days. This last value is in agreement within 8% with the rest-frame $H\alpha$ lag of 20.0 days from our measurement. From the width of the emission line of our spectrum we determine an intrinsic $H\alpha$ line dispersion $\sigma_{line} = 870 km/s$.

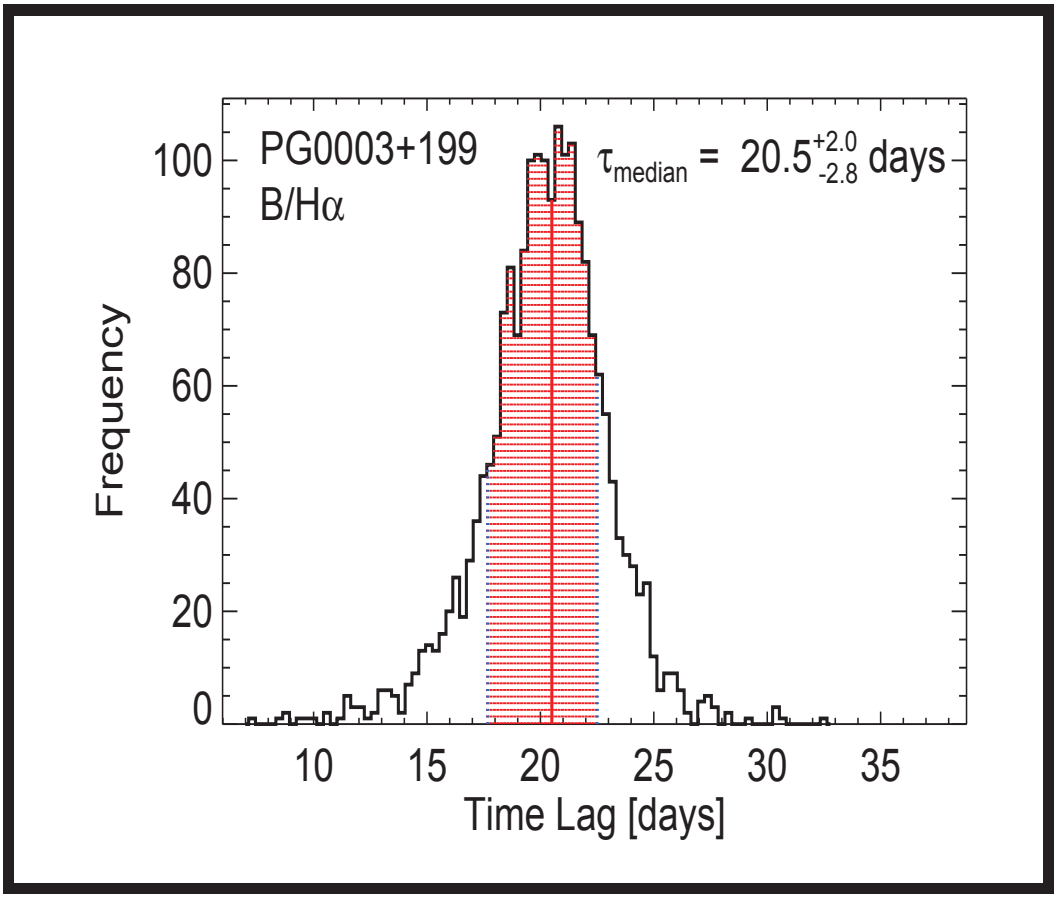

Figure 2.8 .Results of FR/RSS cross correlation for PG0003+199. The histogram shows the distribution of the centroid lag obtained by cross correlating 2000 flux randomized and randomly selected subset light curves. The red area marks the 68% confidence range used to calculate the errors of the centroid.

Using the line dispersion results with the rest-frame lag and adopting the factor $f1.0$ we obtained the black hole mass $M_{BH} = 2.8 \pm 1.1 \times 10^6 M_\odot$. This results is consistent with $M_{BH} = 2.8 \pm 0.8 \times 10^6 M_\odot$ derived via spectroscopic reverberation mapping by Peterson et al. (2004).

2.6 Results for Ark120

Fig (2.9) depicts the light curves of Ark 120. The B-band steeply increases by 17% over 10 days in November 2009 with a sharp peak at end of November 2009. From January to March there is a gradual decline to the original flux level. In November the V and NB light curves are similar to that of the B-band, but with smaller amplitude. In contrast to the steep B-band flux increase, the NB flux increase is stretched until January 2010 with amplitude of 12-15% between begin of November and January.

Similar to 3C120, the NB filter contains about 50% continuum and 50% $H\beta$ line emission and therefore we computed a synthetic $H\beta$ light curve. The synthetic $H\beta$ curve still has a remaining variability pattern in Oct-Nov which its seems to be arise from the relicts of the continuum. However, the important result is that compared to November, the flux in January in the synthetic $H\beta$ light curve is 10% higher.

The cross correlations shows a major peak with a lag of 47.7 days as defined by the centroid τ_{cent} in Fig (2.10). In order to calculate the errors on this measurement, we cross correlated the 2000 pairs of subset light curves and computed the centroid τ_{cent} as is shown in Fig (2.11).

The resulting median lag is $48.0^{3.0}_{-3.3}$ days with an uncertainty of 7%. Correcting the mean lag time for the time dilation factor, we obtain a rest frame lag of $\tau_{rest-frame} = 46.5 \pm 3.25$ days. This results is consistent with the lag of 47 ± 10 days obtained with spectroscopic monitoring by Peterson et al. 1998a, 2004 and with the lag range 34-54 days obtained by Doroshenko et al. (1999).

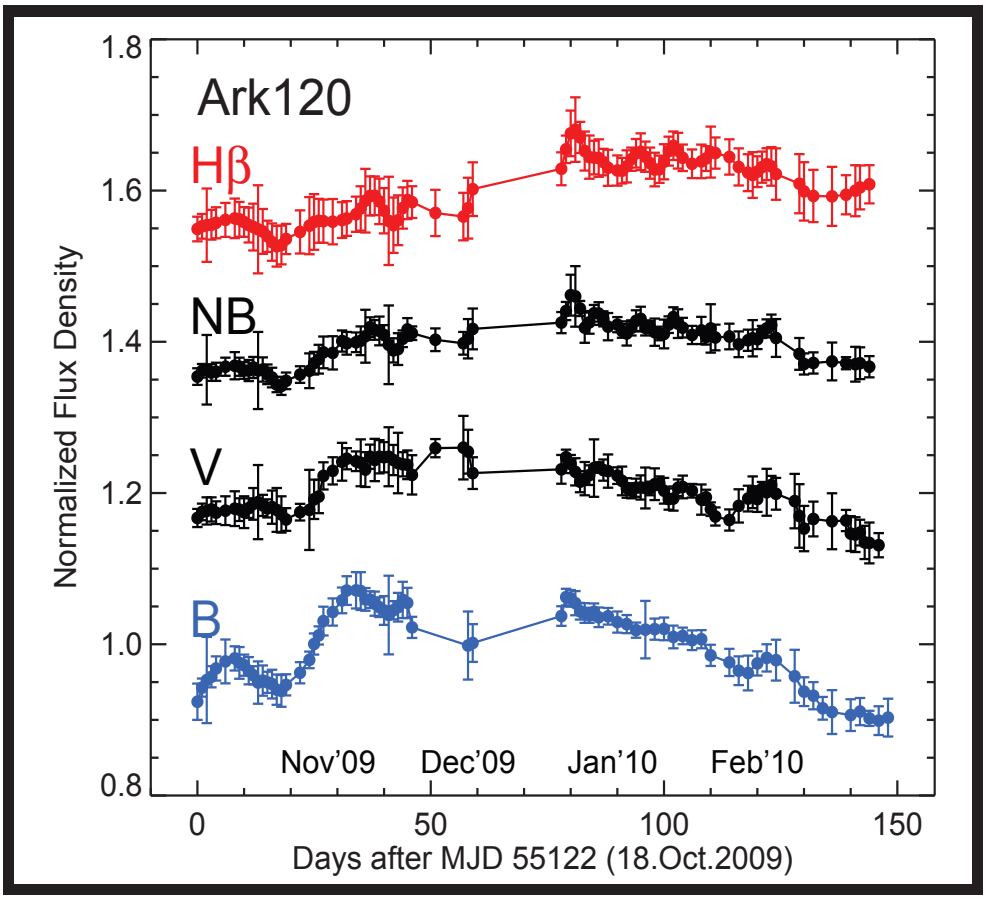

Figure 2.9 .Observed light curves of Ark120 between Oct. 2009 and March 2010. The $H\beta$ light curve is computed by subtracting a scaled V curve from the NB curve and re-normalized to mean = 1. All light curves were shifted from each other by multiples of 0.2 for clarity. The data gap between December 2009 and January 2010 is mostly due to strong winds preventing observations.

From the width of the emission line from our spectrum we determine an intrinsic $H\beta$ line dispersion $\sigma_{line} = 1950 km/s$, this result is in agreement with the value obtained by Peterson et al. (2004). We determined the black hole mass to be $M_{BH} = 34 \pm 12 \times 10^6 M_{\odot}$, consistent with $35 \pm 8 \times 10^6 M_{\odot}$ derived via spectroscopic reverberation mapping by Peterson et al. (2004).

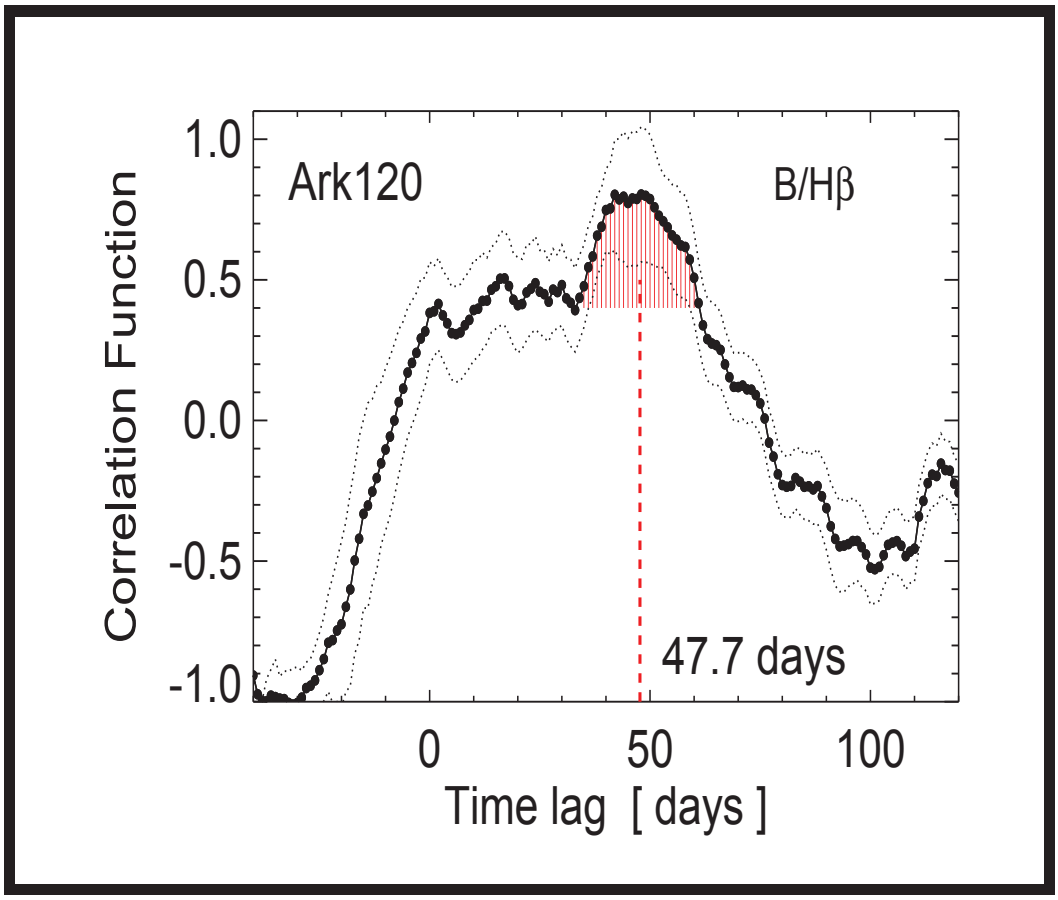

Figure 2.10 .Results of the cross correlations between B and $H\beta$ light curves. The dotted lines indicate the error range ($\pm\sigma$) around the cross correlation. The red area marks the range used to calculate the centroid of the lag, which is represented by the vertical red dashed line.

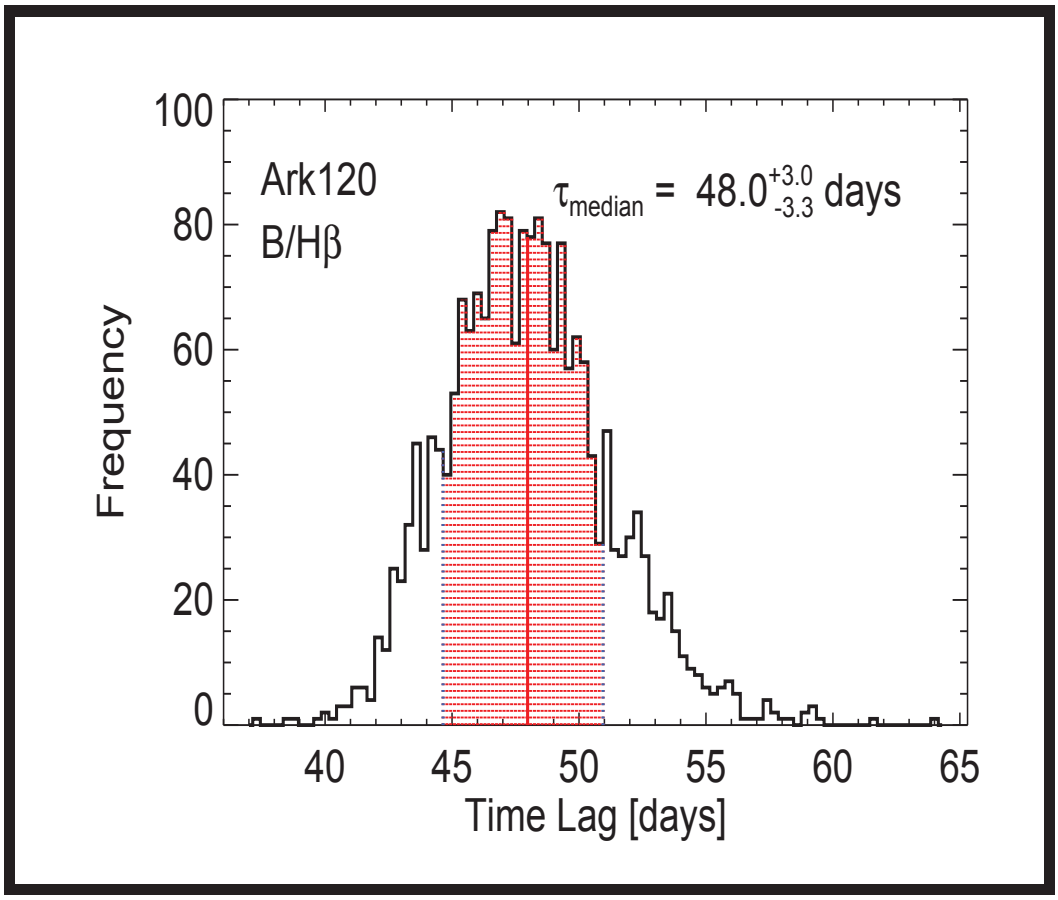

Figure 2.11 .Results of FR/RSS cross correlation for Ark120. The histogram shows the distribution of the centroid lag obtained by cross correlating 2000 flux randomized and randomly selected subset light curves. The red area marks the 68% confidence range used to calculate the errors of the centroid.

2.7 Discussion and Conclusions

We have presented a new photometric reverberation mapping result for 3C120, PG0003+199 and Ark120. For these three objects we obtained lag times, the size of the BLR and the mass of the super-massive black hole. Our results are consistent with previously published results. For 3C120 we considerably improved the measured time lag. Using the host galaxy subtracted AGN luminosity obtained in Chapter 1 and the sizes of the BLR obtained in Chapter 2 we re-analyze the $R_{BLR} - L$ relationship.

This relationship was established using spectroscopic reverberation mapping results, and Bentz et al. (2009) determined a slope of $\alpha = 0.519^{0.063}_{-0.066}$.

In Fig (2.12) we plotted the values obtained by Bentz et al. (2009) for the range appropiate for the objects in this study. One can see the relationship, although many objects have a large uncertainty in the measurements. Our new results place the objects closer to the dashed line representing the best fit slope obtained by Bentz et al. (2009). We should note that the luminosity of 3C120 was low during our observations. 3C120 has shifted away from the slope, but the error bars are smaller than previous results.

We conlude that the previous large dispersion in the R_{BLR}-L relationship is caused by uncertainties in the host-subtracted AGN luminosities and by uncertainties in the R_{BLR} measurements. Our results demonstrate the feasibility of photometric reverberation mapping and offer the possibility to efficiently measure the BLR size, black hole mass and host-subtracted luminosity for hundreds of AGNs, even with small telescopes.

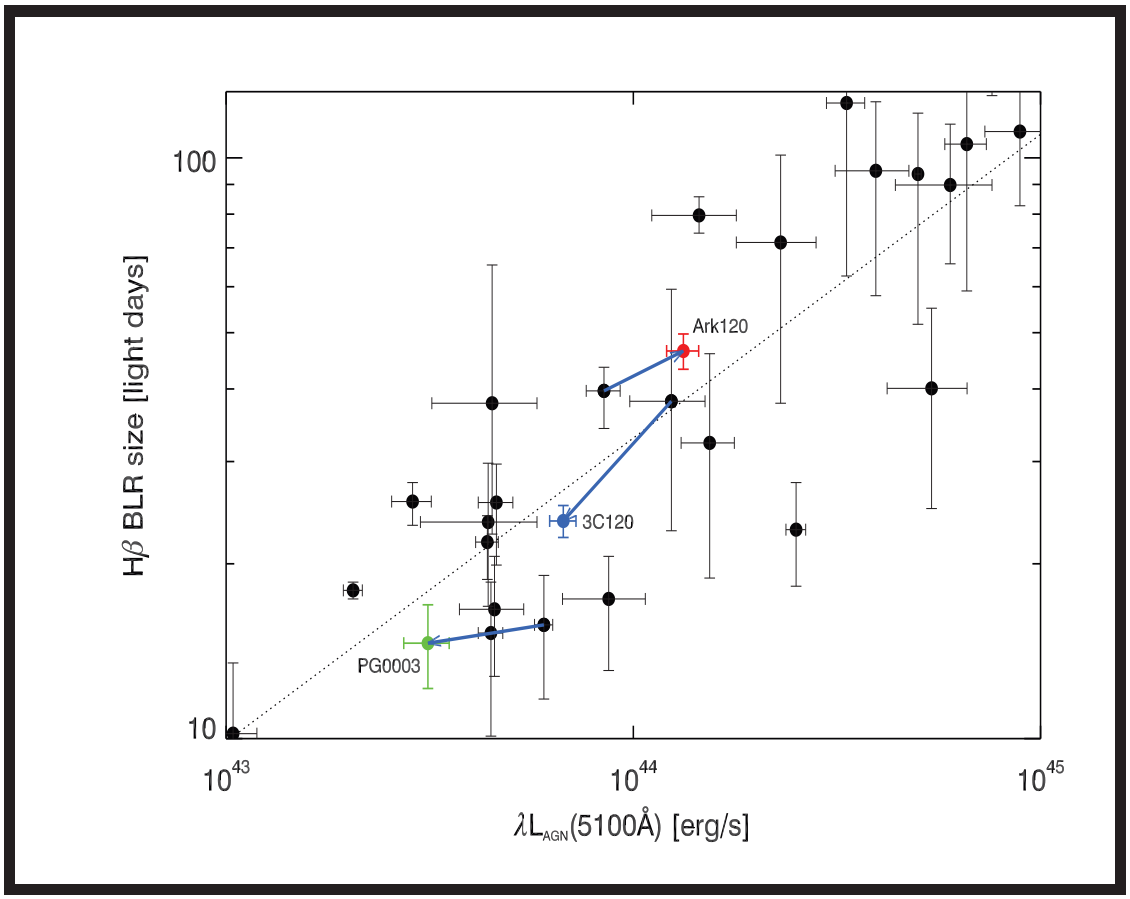

Figure 2.12 . $R_{BLR} - L$ relationship from data of Bentz et al. (2009). Shown is a zoom in containing the objects studied in this work.

Published Work

- Results obtained in Chapter 1 for Ark120 and the results obtained in Chapter 2 for Ark120 and PG0003+199 have been published as Haas.M., Chini,R., Ramolla, M., Pozo Nuñez, F. Westhues, C., Watermann, R., Hoffmeister, V., and Murphy, M: **Photometric AGN reverberation mapping- an efficient tool for BLR sizes, black hole masses and host-subtracted AGN luminosities**. *Astron. Astrophys* (2011).

- We are preparing an article based on the results obtained for 3C120.

Bibliography

[1] Aretxaga, I., et al. On the possible stellar origin of the optical variability of NGC4151. *Mon. Not. R. Astron. Soc.* **269**, 462-474 (1994).

[2] Barway S., et al. Multicolor Surface Photometry of Lenticular Galaxies. I. The Data. *AJ*, **630-646** (2005).

[3] Bentz, M.C, et al. The radius-luminosity relationship for active galactic nuclei: The effect of host galaxy starlight on luminosity measurements.II. The full sample of reverberation-mapped AGNs. *Astrophys. J.* **697**, 160-181 (2009).

[4] Bessell, M.S. UBVRI Photometry II: The cousins VRI System, its temperature and absolute flux calibration, and relevance for two-dimensional photometry. *Astr. Soc. Pacific.* **91**, 589-607 (1987).

[5] Blandford, R.D, et al. Reverberation Mapping of the emission line regions of seyfert galaxies and quasars. *Astrophys. J.* **255**, 419-439 (1982).

[6] Blandford, R.D. Black hole models for active galactic nuclei. *Ann. Rev. Astron. Astrophys.* **22**, 471-506 (1984).

[7] Carini M.T, et al. Microvariability in Seyfert Galaxies. *AJ*, **1811-1816** (2003).

[8] Choloniewski, J. The Shape and Variability of the Nonthermal Component of the Optical Spectra of Active Galaxies. *Acta Astronomica* **31**, 293-311 (1981).

[9] Deeg, H.J., Doyle, L.R. Vaphot- A Package for Precision Differential Aperture Photometry. in proc. of Third Workshop Photometry, Eds. W. Borucki and L.E. Lasher,*NASA/CP-200-209614*, **p.85** 2001.

[10] Doroshenko V.T, et al. $H\beta$ and Continuum Variability in the Seyfert Galaxy Akn120 from Crimean Observations during 1974-1990. *Astronomy Letters*. **25**, 569-581 (1999).

[11] Doroshenko V.T, et al. The Seyfert 1 Galaxy Ark 120 in 1996–2005: *UBVRI* Photometry *Astronomy Rep*. **52**, 167-183 (2008).

[12] Edelson, R.A., Krolik, J.H. The discrete correlation function: A new method for analyzing unevenly sampled variability data. *Astrophys. J.* **333**, 646-659 (1988).

[13] Francis, P.J, et al. A high signal to noise ratio composite quasar spectrum. *Astrophys. J.* **373**, 465-470 (1991).

[14] Hagen-Thorn, V.A. On Choloniewski's Method of Component Separation in the Light of Active Galactic Nuclei. *Astronomy Letters*. **23**, 19-25 (1995).

[15] Hawkins, M.R.S. Gravitational microlensing, quasar variability and missing matter. *Nature* **366**, 242-245 (1993).

[16] Hawkins, M.R.S. Variability in active galactic nuclei: confrontation of models with observations. *Mon. Not. R. Astron. Soc*. **329**, 76-86 (2002).

[17] Horne, K. Five Dimensional Echo-Mapping of AGN Broad-Line Regions. *ASP Conference Series*. **224** (2001).

[18] Howell, Steve B. Two-dimensional aperture photometry - Signal-to-noise ratio of point-source observations and optimal data-extraction techniques. *Astr. Soc. Pacific*, **101**, 612-622 (1989).

[19] Isobe, T., et al. Linear Regression in Astronomy. I. *Astrophys. J.* **364**, 104-113 (1990).

[20] Kaspi, S., et al. Reverberation measurements for 17 quasars and the size-mass-luminosity relations in active galactic nuclei. *Astrophys. J.* **533**, 631 (2000).

[21] Kaspi, S., et al. Reverberation mapping of high-luminosity quasars: First results. *Astrophys. J.* **659**, 997-1007 (2007).

[22] Kawaguchi, T., et al. Optical variability in active galactic nuclei: Starbursts or disk instabilities? *Astrophys. J.* **504**, 671-679 (1998).

[23] Kollatschny W. Accretion disk wind in the AGN broad-line region: Spectroscopically resolved line profile variations in Mrk 110. *Astron. Astrophys.* **407**, 461 (2003a).

[24] Landolt, A.U. UBVRI Photometric Standard Stars Around the Celestial Equator: Updates and Additions. *AJ.* **137**, 4186-4269 (2009).

[25] Lyutyi, V. M. Optical variability of the nuclei of Seyfert galaxies. III - *U*, *B*, *V* observations of 3C 120, II ZW 136, and Arakelyan 120, and the peculiarities of variability in compact galaxies. *Astron. zh.* **56**, 918-927 (1979).

[26] Miller H.R, The optical variability of two Seyfert 1 galaxies: Arkelian 120 and Markarian 231. *Astron. Astrophys.* **35**, 387-389 (1979).

[27] Paczynski, B. Gravitational microlensing at large optical depth. *Astrophys. J.* **301**, 503-516 (1986).

[28] Peng C.Y., et al. Detailed Structural Decomposition of Galaxy Images. *AJ*, **124**, 266-293 (2003).

[29] Peterson, B.M., et al. Continuum and emission-line variability of the Seyfert galaxy Arakelian 120 - Analysis of a large database. *AJ*, **98**, 500-512 (1989).

[30] Peterson, B.M., et al. Optical Continuum and Emission-Line Variability of Seyfert 1 Galaxies. *Astrophys. J.* **501**, 82 (1998a).

[31] Peterson, B.M., et al. On Uncertainties in Cross-Correlation Lags and the Reality of Wavelength-dependent Continuum Lags in Active Galactic Nuclei. *Astr. Soc. Pacific.* **110**, 660 (1998b).

[32] Peterson B.M. Multiwavelength Monitoring of Active Galactic Nuclei. *Astr. Soc. Pacific*, **224** (2001).

[33] Peterson, B.M., et al. Central masses and broad-line region sizes of active galactic nuclei.II. A homogeneus analysis of a large reverberation-mapping database. *Astrophys. J.* **613**, 682-699 (2004).

[34] Rees, M.J. Black hole models for active galactic nuclei. *Ann. Rev. Astron. Astrophys.* **22**, 471-506 (1984).

[35] Riess, A.G., et al. Type Ia Supernova Discoveries at $z > 1$ from the Hubble Space Telescope: Evidence for past deceleration and contraints on dark energy evolution. *AJ*, **607**, 665-687 (2004).

[36] Riess, A.G., et al. Type Ia Supernova Discoveries at $z > 1$ from the Hubble Space Telescope: Evidence for past deceleration and contraints on dark energy evolution. *AJ*, **607**, 665-687 (2004).

[37] Sakata, Y., et al. Long-Term optical continuum color variability of nearby active galactic nuclei. *Astrophys. J.* **711**, 461-483 (2010).

[38] Sandage, A. The redshift-distance relation. IV. The composite nature of N galaxies, their Hubble diagram, and the validity of measured redshifts as distance indicators. *Astrophys. J.* **180**, 687-697 (1973).

[39] Schlegel D.J., et al. Maps of Dust Infrared Emission for Use in Estimation of Reddening and Cosmic Microwave Background Radiation Foregrounds. *Astrophys. J.* **500**, 525-553 (1998).

[40] Schneider, P., et al. A gravitational lens origin for AGN-variability? Consequences of micro-lensing. *Astron. Astrophys.* **171**, 49-65 (1987).

[41] Schneider, P. Upper bounds on the cosmological density of compact objects with sub-solar masses from the variability of QSOs. *Astron. Astrophys.* **279**, 1-20 (1993).

[42] Schneider, P. Detection of (dark) matter concentrations via weak gravitational lensing. *Mon. Not. R. Astron. Soc.* **283**, 837-853 (1996).

[43] Stetson, P. DAOPHOT: A computer program for crowded-field stellar photometry. *Astr. Soc. Pacific.* **99**, 191-222 (1987).

[44] Suganuma, M., et al. Reverberation measurements of the inner radius of the dust torus in nearby Seyfert 1 galaxies. *Astrophys. J.* **639**, 46-63 (2006).

[45] Véron-Cetty, M.P.; Véron, P. A catalogue of quasars and active nuclei: 13th edition. *Astron. Astrophys.* **518**, A10 (2010).

[46] Vestergaard, M. Determining central black-hole masses in distant active galaxies. *Astrophys. J.* **571**, 733 (2002).

[47] Watermann, R. Automatisierte Variabilitätsmessungen im Visuellen und Infraroten. Phd Thesis. Astronomisches Institut Ruhr Universität Bochum (2011).

[48] Webb, J.R., et al. Optical observations of 22 violently variable extragalactic sources- 1968-1986. *AJ*, **95**, 374-397 (1988).

[49] Westhues, C. Diploma Thesis. Astronomisches Institut Ruhr Universität Bochum (2011).

[50] Winkler, H., et al. Variability studies of Seyfert galaxies – I. Broad-band optical photometry. *Mon. Not. R. Astron. Soc.* **257**, 659-676 (1992).

[51] Winkler, H., et al. The extinction, flux distribution and luminosity of Seyfert 1 nuclei derived from UBV(RI) aperture photometry. *Mon. Not. R. Astron. Soc.* **292**, 273-288 (1997).